

MAGNETIC RESONANCE IMAGING OF SACCADIC EYE MOVEMENT CIRCUITRY IN
HEALTHY AND DISEASED STATES

by

DAVID JAMES SCHAEFFER

(Under the Direction of Jennifer E. McDowell)

ABSTRACT

A behavioral hallmark of schizophrenia is poor cognitive control. Cognitive control is a construct which refers to the ability to flexibly respond to changing environments. Saccadic eye movement tasks have emerged as a valuable tool in the cognitive neurosciences for quantifying cognitive control and identifying the neural circuitry related to poor cognitive control in schizophrenia. Although poor cognitive control performance in schizophrenia can be successfully modeled using complex saccadic tasks, a non-trivial proportion of otherwise healthy people from the general population show consonantly poor performance on these tasks. As such, cognitive control ability may be a mediating factor in typical comparisons between healthy groups and people with schizophrenia, with variance in structural and functional differences related to cognitive control rather than illness-specific alterations. This body of work presents a series of functional magnetic resonance imaging (fMRI) and diffusion tensor imaging (DTI) studies aimed at isolating schizophrenia-specific alterations in saccadic eye movement circuitry. Overall, the present findings have utility for clinical neuroimaging studies by demonstrating that functional and structural differences identified between schizophrenia and healthy groups may

not be entirely specific to the disease process and can vary as a function cognitive control capacity in the comparison group.

INDEX WORDS: Cognitive control, Diffusion tensor imaging, Functional magnetic resonance imaging, Saccadic eye movements, Schizophrenia

MAGNETIC RESONANCE IMAGING OF SACCADIC EYE MOVEMENT CIRCUITRY IN
HEALTHY AND DISEASED STATES

by

DAVID JAMES SCHAEFFER

B.S., Michigan Technological University, 2010

A Dissertation Submitted to the Graduate Faculty of The University of Georgia in Partial

Fulfillment of the Requirements for the Degree

DOCTOR OF PHILOSOPHY

ATHENS, GEORGIA

2016

© 2016

David James Schaeffer

All Rights Reserved

MAGNETIC RESONANCE IMAGING OF SACCADIC EYE MOVEMENT CIRCUITRY IN
HEALTHY AND DISEASED STATES

by

DAVID JAMES SCHAEFFER

Major Professor: Jennifer E. McDowell
Committee: Brett A. Clementz
Tianming Liu

Electronic Version Approved:

Suzanne Barbour
Dean of the Graduate School
The University of Georgia
May 2016

DEDICATION

I dedicate this work to my parents Holly and Jim who taught me the value of hard work and to my wife Lauren for her unwavering love and support.

ACKNOWLEDGEMENTS

I would like to express my sincere gratitude to Drs. McDowell and Clementz for being patient and kind mentors and for sharing their wealth of knowledge with me. I would also like to thank Dr. Liu for serving on my dissertation committee and providing valuable technical expertise. Funding for these studies was provided by NIH grants MH001852 and MH094172, the National Science Foundation Graduate Research Fellowship Program, the ARCS Foundation, and the UGA Bio-Imaging Research Center.

TABLE OF CONTENTS

	Page
ACKNOWLEDGEMENTS	v
LIST OF TABLES	viii
LIST OF FIGURES	ix
CHAPTER	
1 INTRODUCTION AND LITERATURE REVIEW	1
Saccadic Eye Movements	3
Neural Substrates of Saccadic Eye Movements.....	5
Alterations of Saccadic Circuitry in Schizophrenia.....	16
2 NEURAL CORRELATES OF BEHAVIORAL VARIATION IN HEALTHY ADULTS' ANTISACCADE PERFORMANCE.....	20
Introduction.....	22
Methods.....	25
Results.....	31
Discussion.....	32
References.....	37
3 WHITE MATTER STRUCTURAL INTEGRITY DIFFERS BETWEEN PEOPLE WITH SCHIZOPHRENIA AND HEALTHY GROUPS AS A FUNCTION OF COGNITIVE CONTROL.....	47
Introduction.....	49

Methods.....	51
Results.....	55
Discussion.....	56
References.....	61
4 WHITE MATTER FIBER INTEGRITY OF THE SACCADIC EYE MOVEMENT NETWORK DIFFERS BETWEEN SCHIZOPHRENIA AND HEALTHY GROUPS.....	71
Introduction.....	73
Method.....	76
Results.....	80
Discussion.....	81
References.....	85
5 DISCUSSION AND CONCLUSIONS.....	94
REFERENCES.....	101

LIST OF TABLES

	Page
Table 2.1: Talairach coordinates of significant BOLD signal change.....	41
Table 3.1: Participant demographics.....	65
Table 3.2: Pearson correlations between voxelwise ROI tracts and CC composite scores	66
Table 3.3: Voxelwise ROI fiber tracts with significant F statistics	67
Table 4.1: Participant demographics.....	90

LIST OF FIGURES

	Page
Figure 1.1: Pattern of fMRI activation associated with a volitional saccade (antisaccade) task ...	19
Figure 2.1: Distribution of percent correct antisaccades from screening session 1	42
Figure 2.2: Stimuli and experimental design for fMRI session	43
Figure 2.3: Hybrid independent component analysis	44
Figure 2.4: Within-group <i>t</i> tests	45
Figure 2.5: Group x Trial Performance interaction	46
Figure 3.1: Voxelwise region of interest analysis and results	68
Figure 3.2: Voxelwise region of interest results	69
Figure 3.3: Fibers of the SLF from a representative subject	70
Figure 3.4: Within-group <i>t</i> tests	71
Figure 3.5: Group x Trial Performance interaction	72
Figure 4.1: Transformation of fMRI regions of interest from Talairach space to DTI space.....	91
Figure 4.2: Brain and behavior correlations	92
Figure 4.3: Fiber tracking between putamen and medial FEF.....	93

CHAPTER 1

INTRODUCTION AND LITERATURE REVIEW

Schizophrenia is a devastating disorder that is characterized by a complex constellation of clinical symptoms. As defined by the *Diagnostic and Statistical Manual of Mental Disorders* (5th ed.; *DSM-5*; American Psychiatric Association, 2013), the contemporary standard for classification of mental disorders, schizophrenia is characterized by positive (e.g., hallucinations or delusions) and negative (e.g., affective flattening or anhedonia) symptoms. Recently, researchers have begun to question the validity of the DSM diagnostic scheme for schizophrenia, citing that the DSM's disease construct may not be biologically valid, with current neurobiological evidence accounting for little variance in schizophrenia symptomatology (Keshavan, Clementz, Pearlson, Sweeny, & Tamminga, 2013). In order to better understand the pathophysiology of schizophrenia, it is necessary to study the biological substrates of the disorder. Neuroimaging studies have demonstrated a number of structural and functional brain abnormalities in schizophrenia, but the relationships between these abnormalities and schizophrenia symptomatology are diverse. A potential method for identifying conformity among these results is to consider brain alterations in context of a well-studied circuitry that has long been reported to show dysfunction in schizophrenia. The saccadic eye movement system is ideally suited to for this task, as a long line of evidence has reliably demonstrated alterations of saccadic circuitry that relate to a hallmark cognitive deficit in schizophrenia – poor cognitive control (see Hutton & Ettinger, 2006 for review).

Cognitive control is a construct which refers to the ability to flexibly respond to changing environments – it is a supervisory process involved in tasks such as attention, internal goal representation, and suppression of irrelevant responses (Alvarez & Emory, 2006). Saccadic eye movement tasks have emerged as a valuable tool in the cognitive neurosciences for quantifying cognitive control and identifying the neural circuitry related to poor cognitive control in schizophrenia. Saccadic tasks range from visually-guided saccades (e.g., prosaccades), which can be best described as reflexive-like movements toward a stimulus, to more cognitively complex movements (e.g., antisaccades). In prosaccade tasks, participants fixate on a central stimulus, and then look toward a cue which appears in the periphery. When participants are asked to look away from the cue (e.g., antisaccade tasks; Hallett, 1977), however, the difficulty of the task increases and additional neural resources are required to suppress the reflexive glance toward the cue. The inability to recruit these additional neural resources is construed as a failure of cognitive control and results in poor task performance (Ford, Goltz, Brown, & Everling, 2005; McDowell, Dyckman, Austin, & Clementz, 2009). Studying the neural correlates of these failures provides insight into malfunctioning circuitry underlying poor cognitive control in schizophrenia.

Although poor cognitive control performance in schizophrenia can be successfully modeled using complex saccadic tasks, some otherwise healthy subjects from the general population show poor performance on these tasks (albeit not as poor as SZ; Hutton & Ettinger, 2006). Functional magnetic resonance imaging (fMRI) studies of antisaccade performance implicate similar frontal and parietal regions with worse antisaccade error rates (i.e., lower cognitive control) in both healthy and schizophrenia samples, with less frontal and parietal activation associated with higher antisaccade error rates (Camchong et al., 2006; Dyckman et al.,

2007; Ford & Everling, 2009; Tu et al., 2010). The underlying neural structure supporting efficient functional communication is also affected. Diffusion tensor imaging (DTI) evidence suggests that deficits in cognitive control in people with schizophrenia are associated with white matter structural substrates across the brain (Liu et al., 2013), particularly in frontal and parietal regions (Karlsgodt et al., 2008). Similar frontal and parietal structures are implicated in poor cognitive control in healthy individuals, with lower cognitive control scores linked to lower structural integrity of fronto-parietal connections (Burzynska et al., 2011). Thus, although low levels of cognitive control are a behavioral hallmark of patients with schizophrenia, some healthy subjects from the general population show comparable deficits in cognitive control and the underlying functional and structural substrates. As such, cognitive control ability may be a mediating factor in typical comparisons between healthy individuals and people with schizophrenia, with variance in functional and structural differences related to cognitive control rather than to the disease process of schizophrenia. The purpose of this body of work is to test this hypothesis and to further isolate schizophrenia specific alterations in the saccadic eye movement network through the use of structural and functional neuroimaging.

Saccadic Eye Movements

In daily life, saccades allow for high-resolution processing of visual scenes by rapidly bringing areas of the visual field onto the fovea (Goldberg & Wurtz, 2013). Saccadic eye movements occur frequently (over 100,000 per day) and are stereotyped, meaning that they are reliably and repeatedly evoked with similar characteristics (e.g., gain, spatial error, latency, and error rate; Abrams, Meyer, & Kornblum, 1989; Duchowski, 2007; Ettinger et al., 2003). Because of these properties, saccades have been adopted experimentally by neurologists and neuroscientists to study the integrity of the neural circuitry underlying a range of eye movement

behaviors (Hutton & Ettinger, 2006). As stated in the above, saccadic tasks range from visually-guided saccades (e.g., prosaccades) to more cognitively complex movements (e.g., antisaccades). The aim of this body of work is to probe the neural correlates of cognitive control, and thus will focus on antisaccade performance. Correct antisaccade performance requires suppression of a prosaccade toward a peripheral visual cue and the generation of a saccade away from the cue (Hallett, 1978). An initial glance towards the cue constitutes an error and is construed as a failure to instate cognitive control.

In the healthy adult population, antisaccade error rate means recur around 20-25% and exist in a unimodal, normal distribution (Calkins, Curtis, Iacono, & Grove, 2004; Evdokimidis et al., 2002; Taylor & Hutton, 2007). Standard deviations of antisaccade error rates are as great as 17% (Evdokimidis et al., 2002), and range from 0 to 29% (Everling & Fischer, 1998); it should be noted that variants of task presentation (e.g., gap vs. step versions) can produce variability in error rates (Hutton & Ettinger, 2006). In the lower tail of this distribution exists a subgroup of the normal population that is otherwise healthy but show error rates similar to patients with schizophrenia (people with schizophrenia show error rates from around 25% to 70%; Cutsuridis, Kumari, & Ettinger, 2014; Fukushima et al., 1988; Hutton & Ettinger, 2006). This poorly performing healthy subgroup is of particular interest in this document, as comparisons between a poorly performing healthy group and a group with schizophrenia would allow for testing of nuanced differences in neural circuitry supporting poor cognitive control between the two groups. Comparing the neural circuitry between these two groups is the crux of this work, as outlined below following the review of saccadic circuitry.

Neural Substrates of Saccadic Eye Movements

Non-human primate models have contributed much of the detail to our current understanding of the saccadic eye movement network (via invasive electrophysiological recordings and anatomical/lesion studies). In humans, lesion studies have been historically the most important (Leigh & Zee, 2006), but the majority of human research has focused on utilizing functional neuroimaging, including positron emission tomography (PET), electro- and magnetoencephalography (EEG & MEG), and fMRI. Although the basic saccade related circuitry identified with these four methodologies is generally convergent (Munoz & Everling, 2004), fMRI saccade studies have increased with the greatest rapidity over the past twenty years (McDowell, Dyckman, Austin, & Clementz, 2008). While task-based functional imaging studies have been informative, a relatively recent advance in MRI methodology, DTI, has the potential to greatly enhance models of saccadic control by characterizing white matter connections between saccade-related regions. Below is a review of the functional and structural neural circuitry of saccadic eye movement generation.

The brain circuitry underlying the generation of saccadic eye movements has been extensively studied in non-human primates since the mid 1970's (Girard & Berthoz, 2005; Holzman, Proctor, & Hughes, 1973). In recent years, functional neuroimaging has provided data which suggests mostly analogous circuitry in humans (Munoz & Everling, 2004). For visually-guided saccades, a number of cortical and subcortical regions have been identified (see Figure 1.1 for fMRI activation of saccadic circuitry), including striate and extrastriate cortices, intraparietal sulcus (IPS), frontal eye fields (FEF) and supplementary eye fields (SEF), and dorsolateral prefrontal cortex (PFC; DeSouza, Menon, & Everling, 2003; Dyckman, Camchong,

Clementz, & McDowell, 2007). Subcortically, the network includes thalamus, basal ganglia, and superior colliculus (SC; Leigh & Kennard, 2004).

Neural substrates of visually-guided saccades. In a typical visually-guided saccadic task, a participant fixates on a central visual cue and then generates a prosaccade toward a cue when it jumps to the periphery. fMRI evidence in humans demonstrates that the visual stimulus (i.e., the target) is first registered and mapped by primary visual cortex, where it is coded retinotopically, with a strong contralateral bias (Geng, Ruff, & Driver, 2009). From primary visual cortex, information is sent to extrastriate visual regions (V2/V3). Extrastriate visual regions are consistently activated in saccadic fMRI experiments and likely play a role in mapping of visual space (Dyckman et al., 2007; Merriam, Genovese, & Colby, 2007).

Multiple imaging modalities confirm that the retinotopically defined visual position information is sent to multiple parietal regions where the processing of a saccadic response can continue (Greenlee, 2000). Regions of parietal cortex are consistently activated in fMRI studies (DeSouza et al., 2003; Dyckman et al., 2007; Ford et al., 2005). Transcranial magnetic stimulation (TMS) of posterior parietal cortex affects both latency and vergence of visually guided saccades, suggesting a role in coordinating the direction of the saccade (Kapoula, Isotalo, Müri, Bucci, & Rivaud-Péchoix, 2001).

The functional role of the FEF has been tested via electrophysiological, lesion, and functional neuroimaging studies in humans. Electrophysiological stimulation in humans shows that microstimulation at any site on the FEF triggers a saccade of a specific direction and amplitude (Blanke & Seeck, 2003). Patients with lesions of the FEF show increased saccade triggering latency (Leigh & Zee, 2006). In fMRI data, greater pre-stimulus BOLD activation in FEF correlated with faster saccadic triggering (Connolly, Goodale, DeSouza, Menon, & Vilis,

2000). Taken together, these studies suggest that FEF is involved in the triggering of intentional saccades (Blanke & Seeck, 2003; Connolly, Goodale, DeSouza, Menon, & Vilis, 2000; Pierrot-Deseilligny, Milea, & Mu, 2004).

The function of the SEF has also been explored through a variety of experimental techniques. Direct microstimulation of SEF in monkeys will generate saccades, but with longer latencies, suggesting common connections among the SEF and FEF (Schlag & Schlag-Rey, 1987). TMS and lesions of SEF in humans severely impair the ability to carry out learned sequences of saccades (Gaymard, Pierrot-Deseilligny, & Rivaud, 1990; Müri, Rösler, & Hess, 1994). Human fMRI studies show SEF activation during prosaccades (Dyckman et al., 2007) and sequences of memory guided saccades (Heide et al., 2001), with greater SEF activation is elicited by more complex sequences of saccades. Overall, these studies suggest that SEF is involved in coordinating sequences of saccades.

For methodological reasons, sub-cortical regions of saccadic control have received less attention than SEF and FEF in functional neuroimaging literature. These issues mostly relate to the size, location, and signal strength of these regions (Lehéricy et al., 2006; Walter, Stadler, Tempelmann, Speck, & Northoff, 2008). Despite these challenges, some fMRI studies do show saccade-related activation of basal ganglia and thalamus which is usually associated with more complex saccadic paradigms, such as those requiring memory guided saccades (Brown et al., 2004; Camchong et al., 2006). Other neuroimaging evidence for the involvement of basal ganglia and thalamus comes from PET data. PET imaging during self-paced horizontal voluntary saccades made in total darkness show activation of basal ganglia (putamen and globus pallidus) and thalamus (Petit et al., 1993).

Neural substrates of volitional saccades. The circuitry discussed above is common to all types of saccades, but increased activation in this network is observed when participants perform more cognitively complex volitional saccades, such as antisaccades (Dyckman et al., 2007; Hutton & Ettinger, 2006). Additional regions are also recruited for complex saccadic tasks. The antisaccade task requires higher order cognitive control processes – participants first suppress a reflexive saccade toward the cue, and then generate a saccade to the mirror location, which is absent a visual cue (Hallett, 1977). Although response suppression of an eye movement toward the cue has been demonstrated as an important component of antisaccade performance (Leigh & Zee, 2006; Pierrot-Deseilligny et al., 2002), recent evidence suggests that pre-setting a large fronto-parietal network *before* the stimulus appears to play a significant role in correct vs. incorrect antisaccade performance (Drewes & VanRullen, 2011; Hamm et al., 2012). Anticipatory reduction in motor circuitry may predispose the suppression of inappropriate saccades during the antisaccade task.

FMRI studies contrasting activation due to prosaccades versus antisaccades typically show increased recruitment of a fronto-parietal network to support correct antisaccade performance (Ford et al., 2005; see Figure 1.1). Cortically, these regions include posterior parietal cortex (PPC), FEF, SEF, PFC, and anterior cingulate cortex (ACC; Hutton & Ettinger, 2006). One exception is visual cortex, which does not always show greater activation due to antisaccades, with some studies showing decreases in visual cortex BOLD responses in prosaccade versus antisaccade contrasts (McDowell et al., 2002; Raemaekers et al., 2007). Subcortical regions, including basal ganglia and thalamus, also show greater activation due to antisaccades compared to prosaccades (Dyckman et al., 2007; Camchong et al., 2007; Krafft et al., 2013; Matsuda et al., 2004).

In order to correctly perform the antisaccade task, the target vector (i.e., the direction of the intended eye movement) must be inverted sometime between the initial registration of the visual stimulus and the saccadic burst of FEF and superior colliculus (Munoz & Everling, 2004). If not, a saccade will be generated toward the target. Functional neuroimaging in humans suggests that the PPC plays a critical role in this vector inversion. Recent meta-analyses of human fMRI and PET data demonstrate that antisaccade trials activated IPS to a greater extent than prosaccade trials (Jamadar et al., 2013; Krafft et al., 2013). Parietal regions may be “pre-set” to preemptively re-map the target vector for antisaccade trials, as demonstrated with EEG – increases in alpha band phase locking have been shown to occur just before correct antisaccade trials, but this effect is absent just prior to error antisaccade trials (Hamm et al., 2012). Consistent with the human imaging evidence, electrophysiological recordings of lateral intraparietal area in monkeys suggests that activity in the lateral intraparietal area switches from the visual direction to the motor direction within 50 ms of the visual signal arriving at lateral intraparietal area (Zhang & Barash, 2000). Overall, these studies suggest that additional activation in parietal cortex during volitional saccades, such as antisaccades, is required to perform vector inversion, allowing for generation of a saccade away from the stimulus.

Functional imaging and lesion data in humans reveal that greater activation in FEF during antisaccades tasks than prosaccade tasks corresponds to differences in the preparatory set required to correctly perform antisaccades. More specifically, event-related fMRI designs indicate that these differences in activation occur prior to the stimulus, rather than just prior to the movement, when FEF sends a motor signal (DeSouza et al., 2003). Further, FEF activity seems to be related to the latency of triggering the correct saccades away from the cue during antisaccade tasks, but not the inhibition of reflexive saccades toward the cue (Leigh & Zee,

2006). EEG evidence has demonstrated a similar effect, with prefrontally distributed pre-stimulus alpha phase effects (likely originating in FEF) linked to saccadic reaction time (Drewes & VanRullen, 2011). Patients with FEF lesions do not make more errors than their healthy counterparts, but show an increased latency during correct antisaccade movements (Pierrot-Deseilligny et al., 2003).

Increased preparatory SEF activation may reduce the probability of a reflexive prosaccade during antisaccade tasks. Electrophysiological recordings in non-human primates show that SEF neurons fire significantly more before antisaccades than before prosaccades in mixed runs (Schlag-Rey, Amador, Sanchez, & Schlag, 1997), with greater activity corresponding to correct antisaccade generation. Neuroimaging studies in humans typically demonstrate greater SEF activation during antisaccades than prosaccades during both the instruction and movement periods (Curtis & D'Esposito, 2003; DeSouza et al., 2003; Dyckman et al., 2007; Ford et al., 2005). This finding is consistent with a 'winner takes all' model, in which the intensity of saccadic commands (i.e., reflexive command vs. volitional command to the opposite direction) competes, with the strongest signal resulting in behavior (Salzman & Newsome, 1994).

The PFC plays a critical role in programming the antisaccade response. FMRI studies suggest that PFC is recruited in addition to the basic saccadic circuitry during antisaccades and that this increased activation occurs prior to correct antisaccade responses (DeSouza et al., 2003; Ford et al., 2005). EEG evidence suggests alpha/theta oscillations within a prefrontal-occipital network can be used to predict the probability of antisaccade errors (Hamm et al., 2012). This functional imaging evidence is supported by data from patients with lesions to PFC, who show increased antisaccade error rates (Pierrot-Deseilligny, 2003). Overall, these studies suggest that

PFC is involved in predicting correct saccadic movements and distributing signals which inhibit incorrect responses (Leigh & Zee, 2006; Pierrot-Deseilligny et al., 2002).

Direct simulation of ACC in nonhuman primates facilitates the production of correct antisaccades (Phillips et al., 2011). Single unit recordings in monkeys suggest that ACC activity may correspond to monitoring the consequences of saccades, particularly with reward (Ito, Stuphorn, Brown, & Schall, 2003). ACC shows greater activation during antisaccade tasks than during prosaccade tasks (Ford et al., 2005), but this finding is less reliably reported than the other saccade related circuitry. Specifically, it has been suggested that ACC is more active during antisaccade trials, but *when* the ACC becomes active differs between correct and error trials (Ford et al., 2005); during correct antisaccade trials, ACC is more active during the preparatory period, whereas during error trials, the ACC is not more active until the response period. The timing of ACC activation is also supported by EEG recordings suggesting lower pre-trial beta oscillations in ACC prior to antisaccade error trials (Hamm et al., 2012). Based on these studies, the ACC seems to play more of an evaluative role in error responses, rather than an active role in presetting the ocular motor circuitry to make a correct response.

Subcortical regions such as basal ganglia and thalamus have been shown, somewhat infrequently, to be related to volitional saccades in fMRI studies (Brown et al., 2004; Dyckman et al., 2007). The role of these regions in saccade movements, however, is likely understated, given the strong reciprocal connections between cortical areas with basal ganglia and thalamus (Neggers et al., 2012). The basal ganglia, for example, has parallel excitatory and inhibitory loops which preset motor system to make a saccade (Watanabe & Munoz, 2010); these loops are fed by cortical regions and the resultant signals are output to SC and thalamus. Patients with Parkinson's show striatal dysfunction linked to poor antisaccade performance (Chan, Armstrong,

Pari, Riopelle, & Munoz, 2005). Given that basal ganglia and thalamus serve as modulatory connection centers in saccadic circuitry (Watanabe & Munoz, 2010), it is likely that information regarding the role of these regions in saccadic network connectivity will burgeon as connectivity of this network via MRI is explored.

Overall, evidence suggests that increased activation during antisaccade tasks as compared to prosaccade tasks involves recruitment of a large frontal (i.e., FEF, SEF, PFC, ACC) and parietal network (i.e., IPL) which distribute the requisite signals to preset the ocular motor system to perform the task correctly. Although the involvement of these regions is clear, the white matter structural connections underlying the functional interactions between these regions has yet to be extensively explored, despite the availability of techniques well-matched to study these dynamics.

Structural connectivity of the saccadic network. Although connectivity of visual cortex is well defined in non-human primate models, DTI studies have recently provided evidence which demonstrates analogous white matter connections in humans. DTI provides a means for characterizing structural integrity by measuring water diffusion in brain tissue (Jones & Leemans, 2011). By measuring translational motion of water molecules, neuroanatomical structure can be inferred. As water is diffusing in the brain, the microstructural environment (e.g., cell membranes, cytoskeletons, and protein structures; Tanner & Stejskal, 1968) influences its path in a predictable way – collisions with microstructure result in changes in the direction of diffusion. DTI captures these deviations in diffusion by sensitizing the MRI signal to molecular motion. In regions where water can move freely, such as in the ventricles or gray matter, diffusion is largely isotropic – the magnitude of diffusion is equal in all directions. In white matter, however, water diffusion is restricted by neuronal structure and thus tends to diffuse

anisotropically, with the magnitude of diffusion greatest in the direction which is parallel to axons.

Extant human DTI literature is generally consistent with retrograde tracing studies in non-human primates. For example, evidence from tracing in macaques demonstrates direct structural connections between IPS and visual cortex (Lewis & Van Essen, 2000). Similarly, in human fMRI/DTI study, Greenberg and colleagues (2012) identified white matter fiber tracts connecting retinotopically defined areas of the visual cortex to topographic regions of IPS; connectivity between these regions modulated visual attention (as measured by the ability to judge a number as even or odd at a specific spatial location, surrounded by distractors). In an MEG/DTI study, faster latencies of peak evoked magnetic fields in occipital cortex showed a positive correlation with FA in fibers linking occipital cortex to PPC and FEFs (Stufflebeam et al., 2008). The authors suggest that increased myelination in these fiber connections corresponds to increased conduction velocity, resulting in faster top-down control and reduced latency of visual evoked responses.

Connectivity of parietal cortex. A probable candidate for facilitating signal transmission between parietal cortex and FEF is the superior longitudinal fasciculus (SLF). SLF connects parietal and frontal lobes and has been associated with visuo-spatial attention and initiation of motor activity in humans (Jang & Hong, 2012). Jang & Hong (2012) traced fibers of SLF from superior parietal lobe directly to the premotor strip of the frontal lobe using DTI tractography. Because the SLF is bidirectional (sharing efferent fibers to and from cortical regions) in humans, it is likely that signals from other prefrontal areas (e.g., DLPFC) send inhibitory signals to PPC via SLF fibers (Makris et al., 2005). Such signals could be hypothesized to modulate top-down control during cognitively complex saccades, with PFC and parietal activation linked to

prosaccade suppression in saccadic fMRI studies (DeSouza et al., 2003; Ford et al., 2005).

Chapters 2 and 3 of this document seek to test such a hypothesis by examining the role of PFC, PPC, and the white matter connections between the two regions in antisaccade error rate.

Evidence of SLF involvement in mediation of signals between IPS and FEF also comes from patients with lesions or reduced integrity of SLF. Patients with SLF lesions show symptoms of unilateral visual neglect, suggesting that an intact SLF plays an important role in transmitting visual attention signals between parietal and frontal cortices (Doricchi & Tomaiuolo, 2003). In children with Williams's syndrome, altered SLF diffusivity is linked to deficits in visuo-spatial processing; these deficits are accompanied by anomalous fronto-parietal functional connectivity (Hoeft et al., 2007). These results indicate that white matter integrity of the SLF mediates visual processing signals between frontal and parietal regions. Understanding the interaction between functional activation and these structural deficits may provide valuable insight into the underlying causes of individual differences in saccadic inhibition.

Connectivity of eye fields. Activation of FEF and SEF (as measured by BOLD fMRI signal) is easily elicited by saccadic paradigms, which can then be defined as seed regions from which white matter fibers can be traced. For example, Neggers et al. (2012) elicited FEF and SEF activation using an antisaccade task and then calculated the probability of connectivity with basal ganglia structures - medial and lateral FEF showed stronger connectivity to putamen than with caudate nucleus, which is in agreement with fMRI evidence showing preferential activation of putamen during antisaccades (Neggers et al., 2012). Other DTI evidence suggests that the human premotor cortex, which is directly anterior of FEF, shows a greater degree of connectivity to putamen than caudate nucleus (Draganski et al., 2008).

In a similar fMRI seed based analysis, de Weijer et al. (2010) reconstructed white matter fiber tracts between FEF, caudate nucleus, and SC. The authors extracted the fMRI time course for each of the FEF seed regions and found that greater FEF activation during antisaccades was more correlated with the FEF-SC pathway than the FEF-striatal pathway. These findings suggest that activation along the FEF-SC pathway is associated with direct generation of saccades, whereas the striatal pathway may serve a gating function. These data are consistent with evidence of direct and indirect loops which preset motor circuits to make either a reflexive or volitional behavior (Watanabe & Munoz, 2010). Overall, fMRI seed based studies have provided valuable information about connectivity between FEF, SEF, and basal ganglia structures related to saccadic function. Studying these fiber pathways in patients with disorders characterized by striatal dysfunction (e.g., Parkinson's disease) could yield interesting and valuable results. Chapter 4 of the present document explores the role of these pathways in schizophrenia.

Connectivity of PFC. FMRI studies show that the PFC plays an important role in error rate during complex saccades (Dyckman et al., 2007; Ford et al., 2005) and suggest that communication between PFC and parietal cortex is vital to this effort. Because SLF is the main conduit of communication between PFC and parietal cortex, white matter fibers of the SLF likely transmit the inhibitory signals between these two regions (Makris et al., 2005). Disruption (via lesion or TMS) at the PFC end of the SLF results in decreased inhibition during antisaccade tasks (i.e., more errors; Pierrot-Deseilligny et al., 2003; Tanji, 2001). Overall, fMRI and DTI studies suggest that the ability to successfully recruit regions involved in cognitive control is not only a function of the magnitude of activation in the region, but is also dependent on the integrity of the underlying white matter network.

In sum, DTI has allowed for significant progress to be made in mapping the white matter connections of the saccadic eye movement system in humans. DTI studies have provided evidence consistent with animal and human lesion studies to suggest that decreased integrity of fronto-parietal and fronto-striatal white matter tracts relates to alterations in saccadic performance. Reduced integrity of these pathways may be the result of deficits in myelination or axonal coherence, resulting in slower neural transmission speeds between regions involved in functional saccadic processing (Song et al., 2002). How decreased integrity in these tracts relates to functional activity in saccade related regions, however, has not yet been extensively explored.

Alterations in Saccadic Circuitry in Schizophrenia

In prosaccade tasks, patients with schizophrenia perform similarly to healthy controls, making few errors and have similar response latencies under most experimental conditions (Fukumoto-Motoshita et al., 2009; Lipton, 1981; Müller, Riedel, Eggert, & Straube, 1999). In antisaccade tasks, however, people with schizophrenia make more errors than their healthy counterparts (Calkins et al., 2004; Cutsuridis et al., 2014; Fukushima et al., 1988) and latencies of correct saccades in schizophrenia are increased (Hutton & Ettinger, 2006). Antisaccade errors are typically construed as a failure to suppress the erroneous reflexive response toward the cue or a failure in generating a response away from the cue (Curtis & D'Esposito, 2003; Cutsuridis et al., 2014; Everling & Fischer, 1998). Otherwise healthy first degree relatives of people with schizophrenia also show increased antisaccade error rates, suggesting heritability and that disrupted performance is not due to other factors such as medication (McDowell, Myles-Worsley, Coon, Byerley, & Clementz, 1999). These failures are likely mediated by dysfunction

of PFC and the cortical and subcortical networks which support it (Fukumoto-Motoshita et al., 2009; Goldman-Rakic, 1994).

Evidence from multiple functional imaging modalities suggests that antisaccade performance deficits in schizophrenia are likely mediated by PFC dysfunction and/or its related circuitry. In fMRI studies, schizophrenia show decreased PFC BOLD contrast during antisaccade tasks compared to healthy control subjects (Camchong et al., 2006; Fukumoto-Motoshita et al., 2009b; McDowell et al., 2002). PET imaging shows decreased PFC blood flow in schizophrenia during volitional saccade tasks (Nakashima et al., 1994). EEG evidence suggests alpha/theta oscillations within a prefrontal-occipital network can be used to predict the probability of antisaccade errors in healthy subjects (Hamm et al, 2012). This functional imaging evidence is supported by data from patients with lesions to PFC, who show increased antisaccade error rates (Pierrot-Deseilligny, 2003).

Subcortical regions, including basal ganglia and thalamus also show functional alterations during volitional saccadic tasks. Patients with schizophrenia show decreased BOLD activation in basal ganglia during complex saccadic tasks, with decreases in both caudate and putamen (Camchong et al., 2006; Raemaekers et al., 2007). In thalamus, improved volitional saccade performance (ocular motor delayed response task) is associated with increased BOLD in normal participants, but not in schizophrenia participants, suggesting subcortical dysfunction (Camchong et al., 2006). Given that basal ganglia and thalamus have strong reciprocal connections with most of the cortical saccadic circuitry (Watanabe & Munoz, 2010), it is likely that saccadic dysfunction in schizophrenia is the result of network dysfunction, rather than caused by any one region.

In order to study network dysfunction of saccadic circuitry in schizophrenia, it is prudent to consider the integrity of structural connections between cortical and subcortical regions. DTI studies of saccadic circuitry in schizophrenia suggest that white matter integrity of frontal and parietal regions is reduced (Manoach et al., 2007). Manoach et al. (2007) found that reduced white matter integrity underlying ACC, FEF and PPC were associated with increased saccadic latency in schizophrenia. Other DTI studies of cognitive control networks in schizophrenia suggest that SLF white matter integrity is reduced in people with schizophrenia as compared to controls (Karlsgodt et al., 2008). Indices of white matter integrity in SLF are also correlated with cognitive control performance (Karlsgodt et al., 2008). The SLF connects frontal and parietal regions which are structurally and functionally identified as regions mediating cognitive control in healthy samples (Burzynska et al., 2011). As such, FA of the SLF is a strong candidate for mediating cognitive in both patient and healthy groups.

Overall, fMRI and DTI in schizophrenia and healthy samples suggest that the ability to successfully recruit regions involved in cognitive control is not only a function of the magnitude and timing of activation in the region, but is also dependent on the integrity of the underlying white matter network. The following studies sought to test this assertion and to delineate patterns of activation (chapter 2) and/or connectivity (chapters 3 & 4) that are specific to schizophrenia from those that are a function of low levels of cognitive control. Ultimately, understanding how functional and structural substrates interact to result in poor antisaccade performance will help elucidate the mechanisms of poor cognitive control in healthy and diseased states.

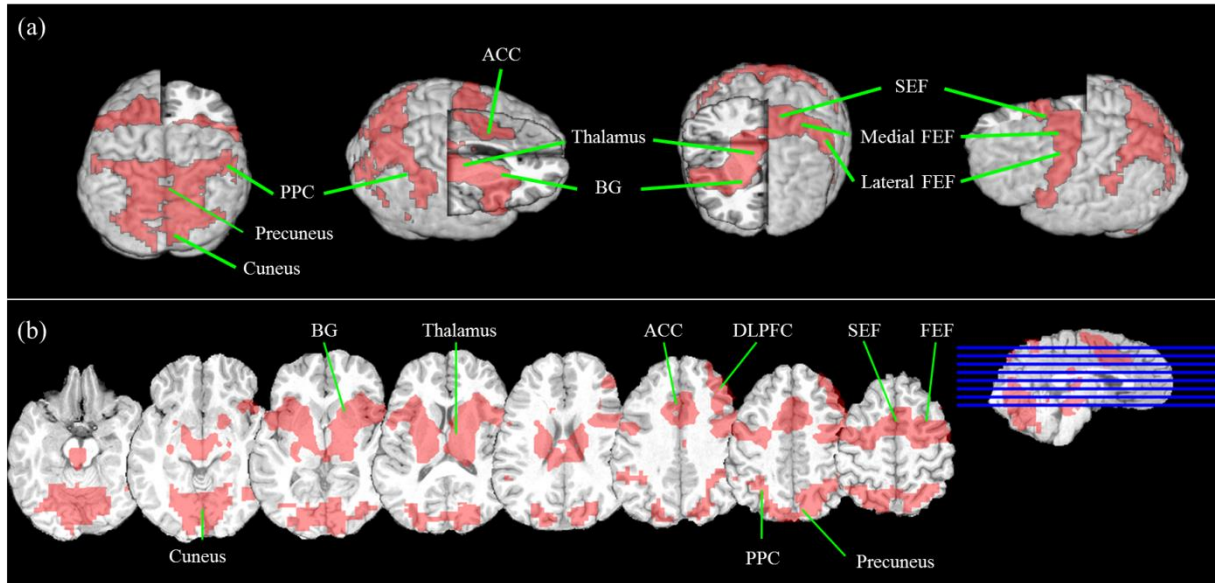


Figure 1.1: Pattern of fMRI activation associated with a volitional saccade (antisaccade) task.

Panel (a) shows saccadic circuitry in red overlaid on a 3-dimensional anatomical rendering at 0, 90, 180, & 270 (left to right) degrees rotation; the right frontal cortex volume is removed to show subcortical saccade circuitry. Panel (b) shows the same circuitry as (a) but is overlaid on axial slices. The blue lines on the sagittal slice (right) indicate the location of the axial slices. In both (a) and (b), the antisaccade related circuitry is based on 13 subjects (adapted from Schaeffer et al., 2013) and overlaid on a representative subject's native space anatomical image. PPC, posterior parietal cortex; ACC, anterior cingulate cortex; BG, basal ganglia; SEF, supplementary eye field; FEF, frontal eye field; DLPFC, dorsolateral prefrontal cortex.

CHAPTER 2
NEURAL CORRELATES OF BEHAVIORAL VARIATION IN HEALTHY ADULTS'
ANTISACCADE PERFORMANCE¹

¹ Schaeffer, D. J., Amlung, M. T., Li, Q., Krafft C. E., Austin, B. P., Dyckman, K. A., & McDowell, J. E. 2013. *Psychophysiology*. 50:325-333.

Reprinted here with permission of the publisher.

Abstract

Cognitive control is required for correct antisaccade performance. High antisaccade error rates characterize certain psychiatric disorders, but can be highly variable, even among healthy groups. Antisaccade data were acquired from a large sample of healthy undergraduates and error rate was quantified. Participants who reliably made few errors ("good" $n = 13$) or many errors ("poor" $n = 13$) were recruited back to perform antisaccades during fMRI acquisition. A data-derived model was used to compare signal between good and poor performers during blocks of antisaccade trials. Behaviorally-derived regressors were used to compare signal between good and poor performers during correct and error trials. Results show differential activation in middle frontal gyrus and inferior parietal lobule between good and poor performers, suggesting that failure to recruit these top-down control regions corresponds to poor antisaccade performance in healthy young adults.

Introduction

Saccades support reflexive-like exploration of our environment via rapid redirection of gaze to center the fovea on an object or place of interest (Leigh & Zee, 2006). In daily life, however, goal directed behavior may require cognitive control to modify reflexive responses. For instance, cognitive control over reflexive saccades can avert gaze from aversive or inappropriate stimuli. As such, evaluating the ability to inhibit reflexive saccades in the face of prepotent stimuli provides a simple and effective index of cognitive control. Antisaccade tasks require the inhibition of a saccade toward a suddenly appearing visual cue and the subsequent generation of a saccade away from the cue (Hallett, 1978). An initial glance *towards* the cue constitutes an error and may be considered a failure to instate cognitive control. High antisaccade error rates characterize certain psychiatric disorders, but error rates can be highly variable, even among healthy groups (Hutton & Ettinger, 2006). This study sought to 1) identify a subset of healthy participants who, based on antisaccade performance, may have difficulty instating cognitive control and 2) characterize that deficit in terms of neural circuitry.

Prosaccades and antisaccades share functional neuroanatomy (for review, see McDowell, Dyckman, Austin & Clementz, 2008); however, changed levels of activation in the basic saccadic circuitry may be required to support antisaccade performance (Hutton & Ettinger, 2006; Munoz & Everling, 2004). When directly compared with prosaccades, antisaccades show increased activation in posterior parietal cortex (PPC), frontal eye fields (FEF) and supplementary eye fields (SEF) (Dyckman, Camchong, Clementz, & McDowell, 2007; DeSouza, Menon, & Everling, 2002; Connolly, Goodale, Goltz, Munoz, 2000).

In addition to differences in the levels of activation within the basic saccadic circuitry, additional regions may be recruited to support the increased cognitive complexity of antisaccade

performance. Of the possible regions involved in antisaccade-related cognitive control, PPC and prefrontal cortex (PFC) seem to play a critical role in correct antisaccade performance.

Specifically, data from nonhuman primate electrophysiology, human lesion, and human functional neuroimaging studies converge to suggest that regions of PPC are involved in the coordinate transformation required for correct antisaccade performance. Recordings of neural activity in PPC of nonhuman primates during pro- and anti-saccades have shown PPC to be active just prior to an antisaccade, suggesting that the PPC encodes the signal to look away from the cue, rather than toward it (Zhang & Barash, 2000). Humans with parietal lobe lesions have displayed impairment in the ability to generate antisaccades, providing further support for the thesis that parietal cortex updates visuo-motor space to allow for movements away from the cue (Sharpe, Cheng, & Eizenman, 2011). Although regions of parietal cortex are important for processing position data for both pro- and anti-saccades, functional neuroimaging has shown that, when compared to prosaccades, blood oxygenation level dependent (BOLD) signal during antisaccades is greater in regions of inferior parietal cortex (Connolly et al., 2000; Krafft et al., in press).

Regions of PFC also have been shown to be involved in correct antisaccade performance. Functional neuroimaging studies comparing pro- and anti-saccades have provided evidence that the PFC shows activation during antisaccade trials, but not prosaccade trials (DeSouza et al., 2002; Dyckman et al., 2007). Other studies suggest a more specific timing from of the PFC, such that activation begins before response generation (McDowell, Kissler, Berg, Dyckman, Gao, Rockstroh & Clementz, 2005), a necessary characteristic for PFC modulation of error avoidance on the antisaccade task. During the period prior to pro- and anti-saccades, the dorsolateral PFC (DLPFC) has shown greater activation for antisaccades, suggesting that the

DLPFC is involved in the preparation necessary to suppress prosaccades toward the cue (DeSouza et al., 2002). Electrophysiological recordings suggest that signals from the PFC suppress unwanted eye movements by modulating the activity of the FEF and superior colliculus (SC) through direct projections to those regions (Johnston & Everling, 2006; Munoz & Everling, 2004). Furthermore, data from electroencephalography (EEG) suggest that prestimulus signals from the PFC modulate correct antisaccade performance by sending top-down signals to visual cortex which function to complement motor preparation in reducing the propensity to glance toward the cue (Clementz, Gao, McDowell, Moratti, Keedy & Sweeney, 2010).

Additional information regarding the functional roles of the PPC and PFC has been provided by studies which dissociate patterns of activation between correct and error antisaccade trials. In an event-related functional magnetic resonance imaging (fMRI) study, Curtis and D'Esposito (2003) demonstrated increased levels of activation in PPC and FEF during correct antisaccade performance not present during antisaccade errors or prosaccade trials. Ford, Glotz, Brown & Everling (2005) compared brain activation during correct and error antisaccade trials and found that activation in frontal and cingulate cortices was associated with correct, but not error antisaccade trials. Taken together, results from the Curtis and Ford studies highlight the requisite role of parietal and frontal activation in correct antisaccade performance.

Although neural deficits associated with poor antisaccade performance have been well documented in clinical populations (for review, see Hutton & Ettinger, 2006), there is a relative dearth of information regarding the neural correlates of poor antisaccade performance in the healthy population. Understanding the neural correlates underlying poor saccadic control within the healthy population may (1) help identify neural circuitry functioning associated with low levels of cognitive control within non-clinical populations and (2) serve as an impetus to explore

failures of cognitive control in other domains, particularly among people who are vulnerable to these types of failures. In healthy adults, for instance, measures of the antisaccade task performance (e.g., percentage of direction errors) have been shown to correlate with cognitive measures of working memory and intelligence domains (Klein, Rauh & Biscaldi, 2010).

By acquiring eye movement data from a large sample of healthy undergraduates, the present study sought to identify both good and poor performing (based on percent of correct responses) subsets of a healthy sample. Once participants were divided into good and poor performing groups, patterns of brain activation corresponding to antisaccade performance were compared. Because poor performers generate a higher proportion of error trials, it was hypothesized that the poor group would show reduced prefrontal (DeSouza et al., 2002; Ford et al., 2005) and parietal (Connolly et al., 2000) activation when compared to the good group. To test for differences between good and poor performers across the blocks of antisaccade trials, a hybrid independent component analysis (ICA; McKeown, 2000) was used. Furthermore, good and poor performers were expected to show differential activation of frontal and parietal regions during correct and error trials (Curtis and D'Esposito, 2003; Ford et al., 2005). The effects of the interaction of Group x Trial Performance were assessed by convolving hemodynamic responses based on correct and error responses separately, then comparing activation patterns correlated with each type of response.

Methods

Participants

A large initial sample ($N = 296$, mean age = 19.3 years, $SD = 1.7$; 60.8% female) of right-handed undergraduate students was recruited through the Psychology Research Pool to participate in this study (see Li et al., 2012 for more information). Participants had no history of

psychiatric illness or severe head trauma via self-report. Two groups, good performers ($n = 13$) and poor performers ($n = 13$), were selected via performance on screening sessions to perform the antisaccade task in the MRI while eye movements were recorded. One participant from each group was omitted from the final analysis due to excessively noisy eye movement data, resulting in 12 participants in each group (good mean age = 19.2 years, $SD = 1.2$, 46.1% female; poor mean age = 19.5 years, $SD = 0.9$, 61.5% female). Groups did not differ on these demographic variables. Participants provided written informed consent and were given course credit or monetary payment for their time. The University of Georgia Institutional Review Board approved this study.

Testing sessions

Sessions 1 & 2. The present study consisted of two behavioral testing sessions and a fMRI session. During sessions 1 & 2, participants completed the antisaccade task while their eye movements were recorded at 500 Hz using an infrared based eye tracking system (Eye Track Model 310; Applied Science Laboratories, Waltham, Massachusetts). A chin rest placed participants 70 cm from a flat color monitor and was used to prevent head movements. A block design was used in which 7 fixation blocks were alternated with 6 antisaccade blocks (8 trials per block). On fixation blocks, participants were instructed to stare at a magenta cue (1° diameter) in the center of the screen. On antisaccade trials, a blue cue (1° diameter) was presented in the center of the screen for a random interval between 1500 ms and 2000 ms (mean duration = 1750 ms). The center cue disappeared, and then after a gap of 200 ms, a blue peripheral cue was presented at $\pm 5^\circ$ or 10° from fixation on the horizontal plane for 1250 ms. A 200 ms gap was used because it has been shown to produce more error trials than non-gap versions of the task (Fischer, Gezeck & Hartnegg, 2000). Participants were instructed not to look at the cue when it

jumped to the side, and to move their eyes to the opposite side of the screen at the same distance from the center.

Eye movement data were analyzed using Matlab (The Mathworks Inc., Natick, Massachusetts). Trials with blinks during stimulus onset and trials with no saccades were eliminated. Eye movement reaction times within 80 ms of peripheral cue onset were excluded, as the movements were likely not in response to the cue. Saccades were scored for direction, latency, and gain. Trials with antisaccade errors (initial saccades made in the same direction of the cue) were scored for error correction (saccades in the opposite direction after a first movement in the wrong direction).

Participants with correct antisaccade performance in the upper ($\geq 80\%$ correct) or lower ($\leq 65\%$ correct) thirds of the distribution in session 1 were invited to return for session 2 (Figure 2.1). If a participant's correct antisaccade score in session 2 remained in the same third of the distribution as it was in session 1, then performance was considered to be reliable. Participants with reliable performance were invited to session 3, during which fMRI data were collected while participants were engaged in the antisaccade task.

Session 3. During session 3, participants completed the antisaccade task in the MRI where functional images and eye movements were recorded simultaneously. FMRI data were acquired using a 3T GE Signa scanner at the UGA Bio-Imaging Research Center (BIRC). During scanning, heads were stabilized by padding and a forehead strap. Eye movements were recorded using a MR compatible eye tracker (MeyeTrack, SensoMotoric Instruments, Inc., Berlin, Germany). A dual mirror system was mounted 16 mm from the participant's nasion on the head coil; one mirror reflected the image of the participant's eye to an infrared camera placed at the rear of the bore, while a second mirror allowed participants to view a projection screen

placed in front of the bore. Eye movements were digitized at 60 Hz and displayed on a computer screen to be monitored by the experimenter during the task. Stimulus presentation was controlled using Presentation software (Neurobehavioral Systems, Albany, California). The stimuli of session 3 (Figure 2.2) were identical to sessions 1 and 2, apart from a central fixation time fixed at 1600 ms and the peripheral cue time of 950 ms. Before entering the scanner, participants were instructed not to look at the cue when it jumped to the side, and to move their eyes to the opposite side of the screen at the same distance from the center. Eye movement data were scored for saccade direction to determine correct or error responses on a trial by trial basis.

During each scan session, two localizer images were taken to ensure accurate whole brain coverage. T1-weighted structural images were acquired axially using spoiled gradient-recall (SPGR) protocol (.9375 x .9375 x 1.2 mm, 150 slices, TR = 7.8 ms, TE = 3 ms, flip angle = 20 degrees, scan time = 6 min 20 sec). For the antisaccade run, T2*-weighted images were acquired using 33 gradient-recalled echo-planar images (3.44 x 3.44 x 4 mm, TR = 2000 ms, TE = 30 ms, flip angle = 90 degrees). To allow for scanner stabilization, 4 images (8 sec scan time) were acquired before the run began; these images were discarded, then image recoding for the functional run began (scan time = 4 min 46 sec). The images were collected obliquely, with the slices aligned to the superior margin of the participants' anterior commissure and the inferior margin of the posterior commissure.

Image analysis

Individual Preprocessing. FMRI analyses were conducted using Analysis of Functional NeuroImages (AFNI; Cox, 1996). Functional EPI data processing began with voxel-wise despiking of the time series data. For each individual, motion correction was done by registering functional volumes to a base volume, which was identified by the following criteria: the median

volume of the longest window of time points with the lowest number of outlier voxels. Functional images were slice time corrected and aligned to T1-weighted anatomical volumes. Each functional volume was then blurred using a 4 mm full-width at half-maximum (FWHM) Gaussian filter. Functional time series were normalized by dividing the signal at each voxel by the mean signal intensity across the entire time series and multiplying the result by 100.

GLM Analyses. This study sought to 1) use a data-derived approach to assess differences between good and poor performers across the blocks of antisaccade trials and 2) use a behaviorally-derived approach to assess differences between good and poor performers on correct and error trials. Thus, two separate GLM analyses were conducted: one data-driven and the other behaviorally-driven.

Data-derived Model. To acquire a model-free task related regressor for the first GLM analysis, a hybrid independent component analysis (ICA) was performed similar to the approach developed by McKeown (2002) and implemented in Dyckman et al. (2007). First, all subjects' preprocessed data were transformed into Talarach space (Talarach & Tournoux, 1998). Second, an averaged dataset was created for input to FSL's MELODIC (Beckmann & Smith, 2004). The ICA yielded 33 spatially independent components. To avoid under- or over-fitting, the number of ICA components was automatically estimated for optimum ICA dimensionality by MELODIC using the Laplace approximation to the Bayesian evidence for the model order. The first component had the same peak frequency as our experimental design and thus was used as a task regressor. Estimates of roll, pitch and yaw (acquired during motion correction) were used as motion regressors. Estimates of motion were obtained from the output matrix of volume registration, which corresponded to the amount of adjustment to roll, pitch, and yaw (in mm) which was needed to register each volume (i.e. TR) to a base volume. The base volume was

chosen by identifying the median volume of the longest window of time points with the lowest number of outlier voxels. Using the coefficients yielded from the ICA based GLM analysis, group level voxel-wise one sample t tests were conducted for the good performers and poor performers to visualize antisaccade task related BOLD signal change. A voxel-wise t test between good and poor performers was performed to test between-group differences in BOLD signal change.

Behaviorally-derived Model. To test for specific trial performance effects, a second analysis was conducted based on individual participant's performance across the task. Eye movement data were scored to identify the response to each trial as either correct or error. Using the time points at which correct or error responses occurred, estimated task related regressors were created by convolving the responses with the hemodynamic response function. Thus, for each participant, we created a correct regressor and an error regressor. Unscorable trials were not modeled in the regressors. Functional images were then transformed into Talaraich space and re-sampled to a resolution of 4 x 4 x 4 mm. For each participant, a GLM analysis was conducted using the correct and error related regressors and the motion regressors discussed in the data-derived model section above. Using the coefficients yielded from the GLM analysis, voxel-wise t tests between correct and error trials were performed to test for within-group differences in BOLD signal change for good and poor performers. A 2 x 2 ANOVA (Group x Trial Performance) was conducted to assess BOLD activation related to correct and error trials for good and poor performers.

To protect against false positives, a clustering method derived from Monte Carlo simulations (accounting for the 4 mm FWHM Gaussian filter and with a connectivity radius of 5.7 mm) was applied to the statistical parametric maps (Ward, 2000). Based on these

simulations, the family-wise alpha of .05 was preserved with an *a priori* voxel-wise probability of .025 and three-dimensional clusters with a minimum volume of 1088 μl (17 or more voxels). Data were clustered using AFNI and resulting statistical parametric maps were used to identify regional BOLD signal changes.

Results

Behavioral Results

The percentage of correct antisaccade trials during session 2 significantly differed between good (mean = 91.8%, $SD = 4.5$) and poor (mean = 53.6%, $SD = 7.0$) ($t = 13.6, p < .05$) performers with useable data from 100% of participants. The group difference persisted at session 3: good (mean = 91.6%, $SD = 4.0$) significantly differed from poor (mean = 60.4%, $SD = 10.3$) ($t = 9.8, p < .05$) performers with usable eye movement data available for 92.3% of participants. Both groups corrected antisaccade errors at a high rate (good = 100.0% and poor = 89.6%).

Independent-samples t tests were conducted to compare reaction times during correct and error trials between good and poor performers. Although reaction times of good performers (mean = 260.2 ms; $SD = 30.4$) were slower than poor performers (mean = 238.4 ms; $SD = 35.4$) during correct trials, differences that did not reach significance; $t(22) = 1.6, p = .11$. Similarly, during error trials, reaction times of good performers (mean = 201.2 ms; $SD = 31.4$) were slower than poor performers (mean = 176.2 ms; $SD = 37.9$), but differences did not reach significance; $t(22) = 1.6, p = .11$. With a much larger sample size, we recently reported (Li et al., 2012) a pattern of good performers showing slower response times in healthy subjects.

Imaging Results

Data-derived Model. Clustered one sample t maps comparing BOLD signal change for each group versus zero were calculated (Figure 2.3). Both groups showed increased BOLD signal change in regions known to be involved in antisaccade performance: SEF, FEF, PPC, frontal cortex, middle occipital gyrus (MOG), striatum, and thalamus. A whole brain, between group t map showed differences between BOLD signal change in good and poor performers (Table 2.1). Good performers showed reduced BOLD signal change in left cuneus. Poor performers showed reduced BOLD signal change in right middle frontal gyrus (MFG), bilateral inferior parietal lobule (IPL), left MOG and left cerebellum.

Behaviorally-derived Model. A whole brain, within group t map comparing correct and error trials in good performers showed greater BOLD signal change in left inferior frontal gyrus (IFG), left middle frontal gyrus and bilateral superior frontal gyrus (SFG) during error trials (Figure 2.4, left). Good performers also showed greater BOLD signal change in bilateral cerebellum. A whole brain, within group t map comparing correct and error trials in poor performers showed greater BOLD signal change in left superior temporal gyrus (STG) and IFG during error trials (Figure 2.4, right).

A whole brain Group x Trial Performance interaction map showed no between group differences on correct trials. Significant differences were observed, however, between good and poor performers on error trials $F(1, 22) = 4.35, p = .05$ (Figure 2.5; see Table 2.1 for Talaraich coordinates). Good performers showed reduced BOLD signal change in right precuneus and right cerebellum as compared to poor performers during errors. Poor performers showed reduced BOLD signal change in two separate right MFG clusters, and in the right IPL compared to good performers during error trials.

Discussion

The main focus of this study was to elucidate the neural correlates of poor antisaccade performance in a subset of healthy young adults. The data derived (ICA) analysis of overall antisaccade performance demonstrated that poor performers ($\leq 65\%$ correct) showed less BOLD signal change in regions involved in top-down cognitive control, compared to good performers ($\geq 80\%$ correct). This study also sought to dissociate activation patterns during correct trials from those during error trials through the use of trial by trial responses on a block design. This behaviorally-derived analysis showed that good and poor performers showed similar patterns of activation on correct trials, but on error trials differential patterns of activation in MFG, IPL, precuneus and cerebellum were observed.

Data-derived model

Across the blocks of antisaccade trials, both good and poor performers showed activation in SEF, FEF, PPC, PFC, MOG, striatum, and thalamus – regions which have been commonly associated with antisaccade performance (McDowell et al., 2008). Poor performers, however, showed a reduction in BOLD signal change in MFG and IPL as compared to good performers. Patterns of reduced frontal activation have been associated with deficits in saccadic inhibition in clinical populations. Patients with schizophrenia, for example, have shown decreased BOLD signal change in MFG and its associated subcortical circuitry during blocks of the antisaccade task when compared to healthy controls (McDowell et al., 2002; Tu, Yang, Kuo, Hsieh & Su, 2006). Reduction of IPL activation among poor performers may represent a failure of sensorimotor transformation required to generate a saccade away from the cue. This is consistent with nonhuman primate neural recordings which suggest that PPC encodes the motor signal to look away from the cue (Zhang & Barash, 2000).

Behaviorally-derived model

Event-related designs have provided evidence for dissociating the neural correlates of correct antisaccade trials from the neural correlates of antisaccade error trials (Ettinger et al., 2008; Curtis & D'Esposito, 2003; Ford et al., 2005). In the present study, good and poor performers showed differential patterns of activation on correct and error trials. When compared within group, both good and poor performers showed greater activation in IFG during error trials. Good performers, unlike poor performers, also showed greater activation in MFG and SFG. In a Group x Trial Performance interaction, poor performers showed reduced activation compared to good performers in MFG and IPL on error, but not correct trials. These results are consistent with the Ford et al. (2005) event-related fMRI study which provided data to suggest that a large frontal and parietal network is involved in preventing errors during the antisaccade task. Here, greater activation in frontal regions and IPL in good performers likely represents an attempt to instate cognitive control during the trial containing the antisaccade error (Clementz, Brahmabhatt, McDowell, Brown & Sweeney, 2007; Sharpe et al., 2011). Poor performers showed similar patterns to good performers on correct trials, but showed greater activation in precuneus and cerebellum on error trials. In poor performers, greater activation in precuneus may represent an uninhibited bottom-up response to the stimuli.

The distinct patterns between good and poor performers during error trials could represent the absence of top-down prefrontal and parietal control in poor performers. Microelectrode and EEG data suggest that the PFC may send top-down inhibitory signals directly to early visual areas, ostensibly preventing saccade errors toward the stimulus (Johnston & Everling, 2006; Munoz & Everling, 2004; Clementz et al., 2010). In addition to the PFC, parietal regions have been shown to play a role in top-down modulation of visual responses.

Patients with parietal lesions show an increased rate of antisaccade errors (Sharpe et al., 2011). Thus, when top-down control regions are not active in poor performers, bottom-up visual regions (e.g., precuneus) are uninhibited, and the likelihood of making an antisaccade error is increased. Conversely, although good performers made errors, their top-down control circuitry was more active during the errors and likely contributed to a reduced probability of a future error.

These results should be interpreted within the context of the following caveats. First, we could not assess the shape of the hemodynamic response associated with correct and error trials. Despite this, we were able to show differences in brain activation between correct and error trials. Because the hemodynamic response has been shown to be linearly additive, individual responses, such as those corresponding to correct and error trials, can be demarcated out of a block of responses, provided that they are more than two seconds apart (Dale & Buckner, 1997). Second, statistical power may have been an issue in the comparison of good and poor performers based on their correct and error trials alone. Because good performers were characterized by more correct trials, the power to predict activation due to correct trials was greater for good performers. Likewise, the power to predict activation due to error trials was greater for poor performers. This, however, did not seem to be an issue in the error trial only comparison; good performers showed greater activation in two regions, MFG and IPL, despite reduced power. Third, activation patterns in poor performers could have resulted from low task engagement, rather than deficits in cognitive control. Poor performers did, however, make correction saccades during most (89.6 %) error trials. Thus, it could be argued that poor performers were engaged in the task, or else they would not have corrected error saccades.

The present findings may have potential utility for studies comparing healthy controls to patient groups. Here, we have identified a poor performing subset of a healthy sample and

shown that this group differs in terms of neural activation patterns from a group who performs well on the antisaccade task. Although sampling good performing healthy participants is convenient, these findings suggest the importance of sampling from a full distribution of performance. Having a particularly well performing control group could bias differences in activation (Hill & Neiswanger, 1996). Thus utilizing control groups that represent the full performance distribution for comparison with patient samples might provide further detail on circuitry specific to the illness, rather than performance.

The results from this study suggest that a failure to activate frontal and parietal regions involved in top-down control corresponds to poor antisaccade performance in healthy young adults. Moreover, these data illustrate that levels of activation in top-down control regions during error trials can differentiate cognitive control ability. Here, poor performing healthy adults were able to activate the same top-down control regions as a good performing subset during correct trials, but showed an absence of the activation in these regions during error trials. Therefore, future work investigating patterns of activation during error trials might help further our understanding of why people vary in their ability to instate cognitive control.

References

- Beckmann, C. F., & Smith, S. M. (2004). Probabilistic independent component analysis for functional magnetic resonance imaging. *IEEE Transactions on Medical Imaging*, *23*, 137-152. doi:10.1109/tmi.2003.822821
- Connolly, J. D., Goodale, M. A., DeSouza, J. F., Menon, R.S., Vilis, T. (2000). A comparison of frontoparietal fMRI activation during anti-saccades and anti-pointing. *Journal of Neurophysiology*, *84*, 1645–55. Retrieved from <http://jn.physiology.org/content/84/3/1645.full>
- Clementz, B. A., Brahmabhatt, S. B., McDowell, J. E., Brown, R., & Sweeney, J. A. (2007). When does the brain inform the eyes whether and where to move? An EEG study in humans. *Cerebral Cortex*, *17*, 2634-2643. doi:10.1093/cercor/bhl171
- Clementz, B. A., Gao, Y., McDowell, J. E., Moratti, S., Keedy, S. K., & Sweeney, J. A. (2010). Top-down control of visual sensory processing during an ocular motor response inhibition task. *Psychophysiology*, *47*, 1011-1018. doi:10.1111/j.1469-8986.2010.01026.x
- Cox, R. W. (1996). AFNI: software for analysis and visualization of functional magnetic resonance neuroimages. *Computers and Biomedical Research*, *29*, 162-173.
- Curtis, C. E. & D'Esposito (2003). Success and failure suppressing reflexive behavior. *Journal of Cognitive Neuroscience*, *15*, 409-418. doi:10.1162/089892903321593126
- Dale, A. M. Buckner, R. L. (1997). Selective averaging of rapidly presented individual trials using fMRI. *Human Brain Mapping*, *5*, 329-340. doi:10.1002/(SICI)1097-0193(1997)5:5<329::AID-HBM1>3.0.CO;2-5
- DeSouza, J. F., Menon, R. S., & Everling, S. (2002). Preparatory set associated with pro-saccades and anti-saccades in humans investigated with event-related fMRI. *Journal of*

- Neurophysiology*, 89, 1016-1023. doi: 10.1152/jn.00562.2002
- Dyckman, K. A., Camchong, J., Clementz, B. A., & McDowell, J. E. (2007). An effect of context on saccade-related behavior and brain activity. *NeuroImage*, 36, 774-784. doi:10.1016/j.neuroimage.2007.03.023
- Ettinger, U., Ffytche, D. H., Kumari, V., Kathmann, N., Reuter, B., Zelaya, F., & Williams, S. C. R. (2008). Decomposing the neural correlates of antisaccade eye movements using event-related fMRI. *Cerebral Cortex*, 18, 1148-1159. doi:10.1093/cercor/bhm147
- Fischer, B., Gezeck, S., & Hartnegg, K. (2000). On the production and correction of involuntary prosaccades in a gap antisaccade task. *Vision Research*, 40, 2211-2217. doi:10.1016/S0042-6989(98)00082-1
- Ford, K. A., Goltz, H. C., Brown, M. R., & Everling, S. (2005). Neural processes associated with antisaccade performance investigated with event-related fMRI. *Journal of Neurophysiology*, 94, 429-440. doi:10.1152/jn.00471.2004
- Hallett, P. E. (1978). Primary and secondary saccades to goals defined by instructions. *Vision Research*, 18, 1279-1296. doi:10.1016/0042-6989(78)90218-3
- Hill, S. Y. & Neiswanger, K. (1997). The value of narrow psychiatric phenotypes and “super” normal controls. *Handbook of Psychiatric Genetics* (Vol. 236). CRC Press: New York.
- Hutton, S. B., & Ettinger, U. (2006). The antisaccade task as a research tool in psychopathology: A critical review. *Psychophysiology*, 43, 302-313. doi:10.1111/j.1469-8986.2006.00403.x
- Johnston, K. & Everling, S. (2006). Neural activity in monkey prefrontal cortex is modulated by task context and behavioral instruction during delayed-match-to-sample and conditional prosaccade-antisaccade tasks. *Journal of Cognitive Neuroscience*, 18, 749-765. doi:10.1162/jocn.2006.18.5.749

- Klein, C., Rauh, R. & Biscaldi, M. (2010). Cognitive correlates of anti-saccade task performance. *Experimental Brain Research*, 203, 759-764. doi: 10.1007/s00221-010-2276-5
- Krafft, C., Schwarz, N., Chi, L., Li, Q., Schaeffer, D., ... & McDowell, J. (in press). The location and function of parietal cortex supporting of reflexive and volitional saccades, a meta-analysis of over a decade of functional MRI data. *Horizons of Neuroscience Research, Volume 9*. Hauppauge, NY: Nova Science Publishers.
- Leigh, R. J., & Zee, D. S. (2006). *The neurology of eye movements* (Vol. 4). Oxford: Oxford University.
- Li, Q., Amlung, M. T., Valtcheva, M., Camchong, J., Austin, B. P., Dyckman, K. A., ... McDowell, J. E. (2012). Evidence from cluster analysis for differentiation of antisaccade performance groups based on speed/accuracy trade-offs. *International Journal of Psychophysiology*, 85, 274-277. doi: 10.1016/j.ipsycho.2012.03.008
- Mazhari, S., Price, G., Dragović, M., Waters, F. A., Clissa, P., & Jablensky, A. (2011). Revisiting the suitability of antisaccade performance as an endophenotype in schizophrenia. *Brain and Cognition*, 77, 223-230. doi:10.1016/j.bandc.2011.08.006
- McDowell, J. E., Brown, G. G., Paulus, M., Martinez, A., Stewart, S. E., Dubowitz, D. J., & Braff, D. L. (2002). Neural correlates of refixation saccades and antisaccades in normal and schizophrenia subjects. *Biological Psychiatry*, 51, 216-223. doi:10.1016/S0006-3223(01)01204-5
- McDowell, J. E., Kissler J. M., Berg, P., Dyckman, K. A, Gao, Y., Rockstroh, B. & Clementz, B. A. (2005). Electroencephalography/magnetoencephalography study of cortical activities preceding prosaccades and antisaccades. *Neuroreport*, 16, 663-668. doi:

10.1097/00001756-200505120-00002

- McDowell, J. E., Dyckman, K. A., Austin, B. P., & Clementz, B. A. (2008). Neurophysiology and neuroanatomy of reflexive and volitional saccades: Evidence from studies of humans. *Brain and Cognition*, *68*, 255-270. doi:10.1016/j.bandc.2008.08.016
- McKeown, M. J. (2000). Detection of consistently task-related activations in fMRI data with hybrid independent component analysis. *NeuroImage*, *11*, 24-35. doi:10.1006/nimg.1999.0518
- Munoz, D. P., & Everling, S. (2004). Look away: the anti-saccade task and the voluntary control of eye movement. *Nature Reviews Neuroscience*, *5*, 218-228. doi:10.1038/nrn1345
- Sharpe, J. A., Cheng, P., & Eizenman, M. (2011). Antisaccade generation is impaired after parietal lobe lesions. *Annals of the New York Academy of Sciences*, *1233*, 194-199. doi:10.1111/j.1749-6632.2011.06178.x
- Talaraich, J., Tournoux, P. (1998). Co-planar stereotaxic atlas of the human brain: a 3-dimensional proportional system, an approach to cerebral imaging. Thieme Medical Publishers, New York.
- Tu, P., Yang, T. H., Kuo, W. J., Hsieh, J. C., & Su, T. P. (2006). Neural correlates of antisaccade deficits in schizophrenia, an fMRI study. *Journal of Psychiatric Research*, *40*, 606-612. doi:10.1016/j.jpsychires.2006.05.012
- Ward, B. D. (2000). Simultaneous inference for fMRI data, AlphaSim program documentation for afni: Medical College of Wisconsin, Milwaukee.
- Zhang, M. & Barash, S. (2000). Neuronal switching of sensorimotor transformations for antisaccades. *Nature*, *408*, 971-975. doi:10.1038/35050097

Table 2.1: Talairach coordinates of significant BOLD signal change

	Region	L/R	Center of mass			Cluster size (voxels)
			X	Y	Z	
<u>Good vs. poor performers</u>						
	<u>Good > poor</u>					
	MFG	R	40	22	36	45
	IPL	R	50	-46	33	25
		L	-54	-48	27	34
	MOG	L	-34	-70	-14	81
	Cerebellum	L	-14	-24	-24	27
	<u>Poor > good</u>					
	Cuneus	L	-10	-60	7	43
<u>Error trials</u>						
	<u>Good > poor</u>					
	MFG	R	39	22	23	61
	MFG	R	32	54	3	18
	IPL	R	48	-62	26	52
	<u>Poor > good</u>					
	Precuneus	R	13	-46	58	23
	Cerebellum	R	12	-39	-37	42

Note. MFG = middle frontal gyrus; IPL = inferior parietal lobule; MOG = middle occipital gyrus.

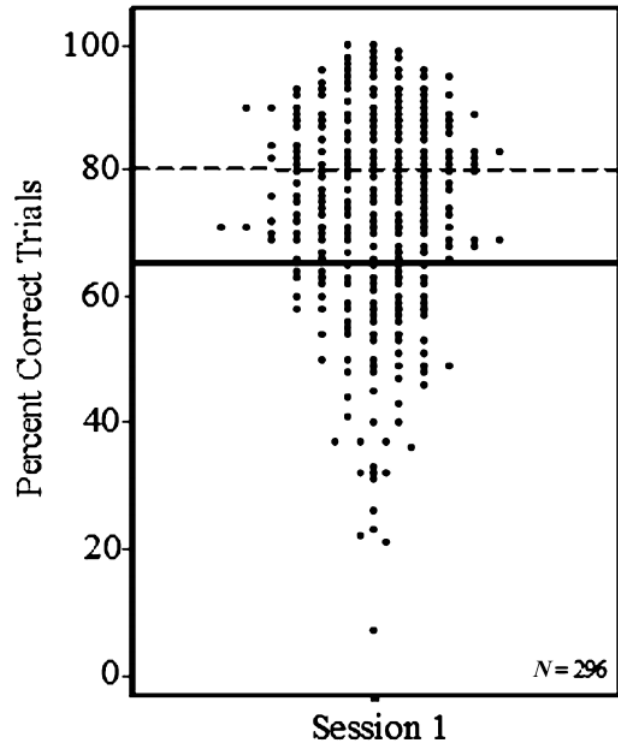


Figure 2.1: Distribution of percent correct antisaccades from screening session 1 ($N = 296$). Lines represent upper and lower third cutoff points; good performers were defined as scoring above 80% (dashed line) correct and poor performers below 65% (solid line).

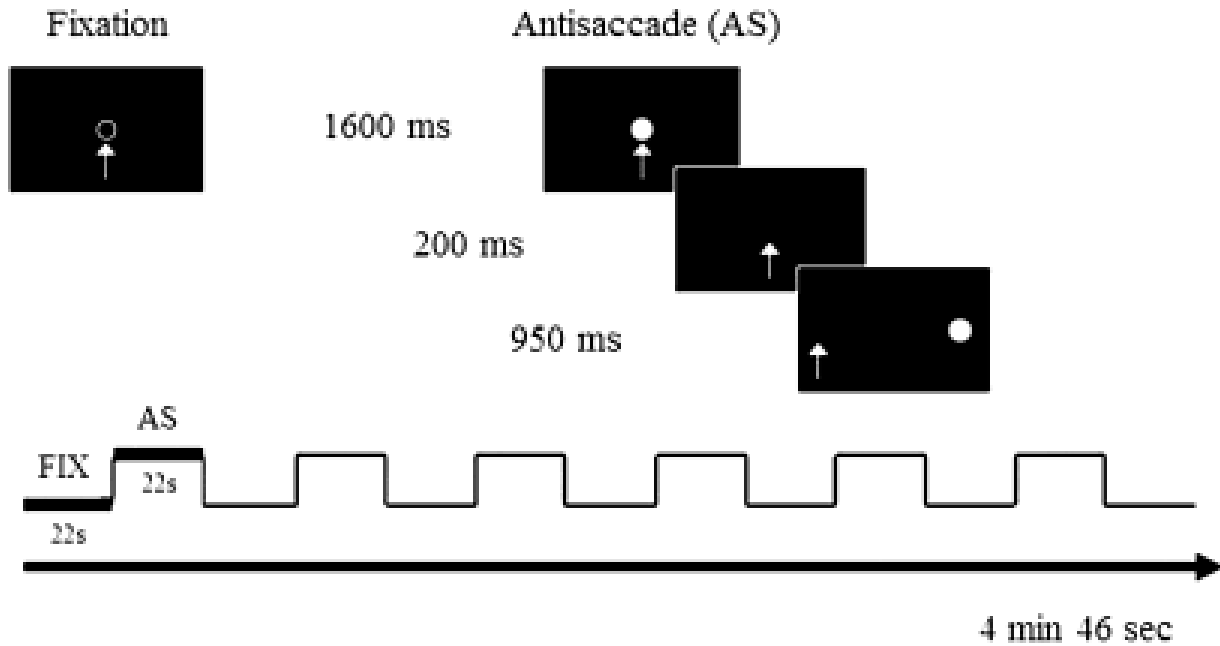


Figure 2.2: Stimuli and experimental design for fMRI session. The arrow indicates where the participant should look for each stimulus presentation. The run consisted of seven fixation blocks alternated with six blocks consisting of eight antisaccade trials. During the experiment, the fixation and antisaccade cues were presented as magenta and blue, respectively.

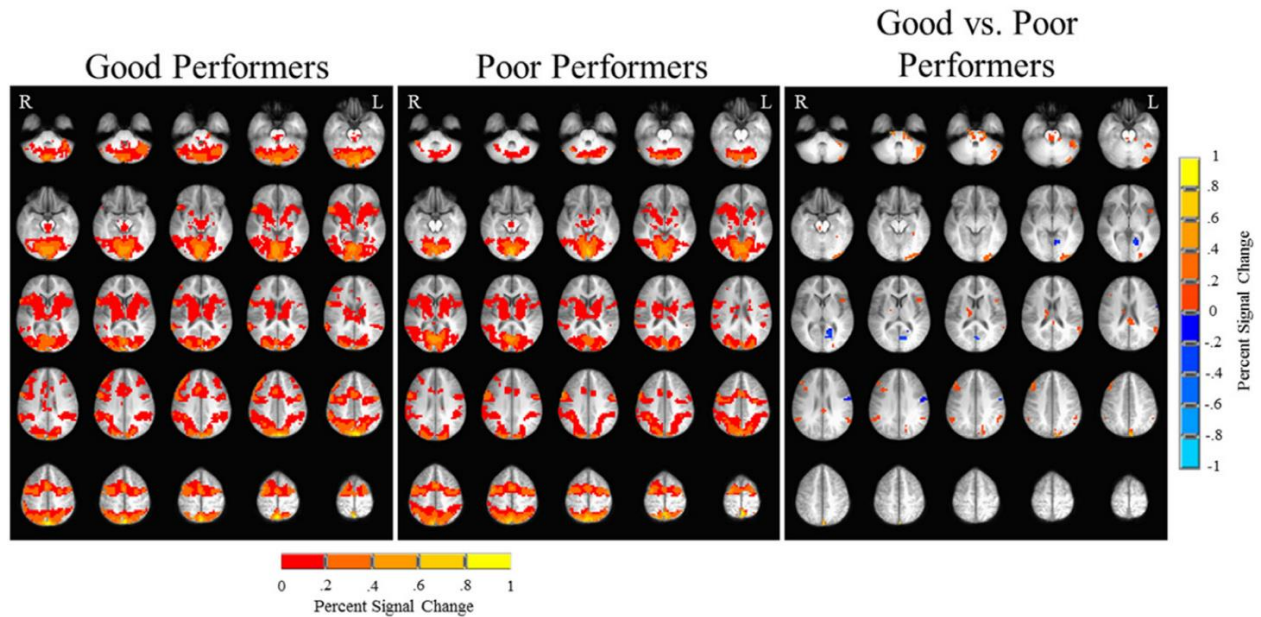


Figure 2.3: Hybrid independent component analysis. Axial slices ($z = -35$ through $z = 62$, functional slice thickness = 4mm) displaying activation significant at $\alpha = .05$ (corrected). The left image (good performers) and center image (poor performers) show one sample t tests for activation related to the first ICA component. In the right image, a t test between good and poor performers shows greater activation for good performers (warm colors) and poor performers (cool colors). The underlying anatomical image was averaged across groups. Image displayed in radiological convention.

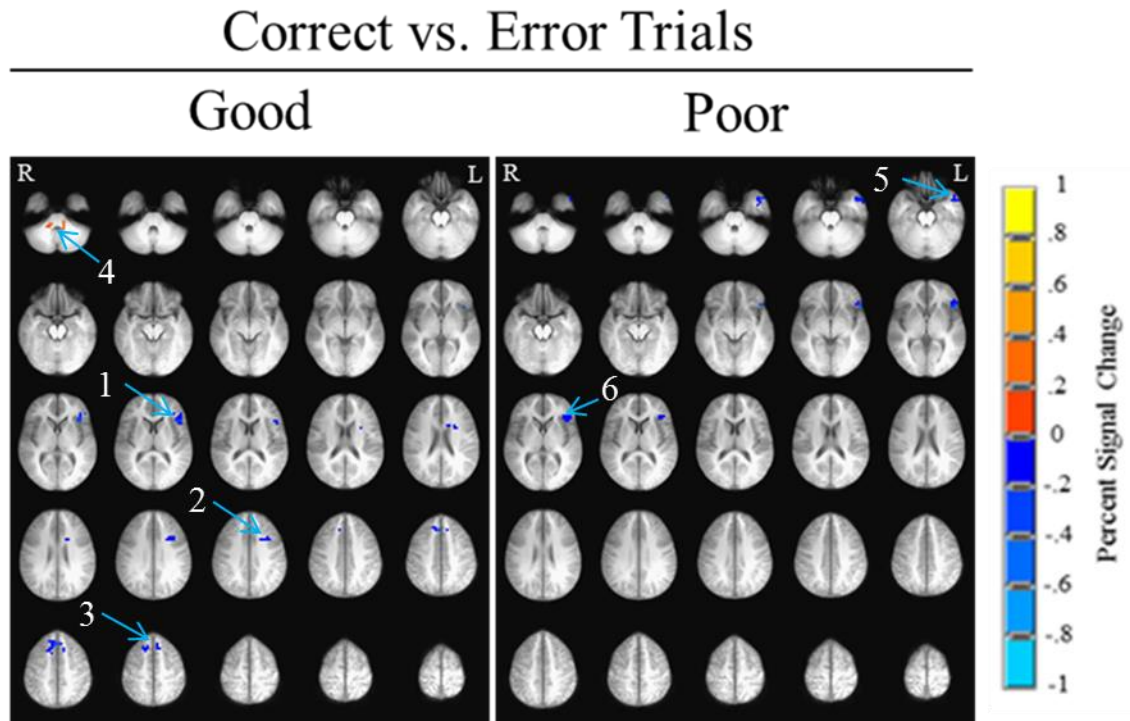


Figure 2.4: Within group t tests. Axial slices ($z = -35$ through $z = 62$, functional slice thickness = 4mm). The left image (good performers) and right image (poor performers) display activation significant at $\alpha = .05$ (corrected) for within group t tests between correct and error trials. Cooler colors represent greater activation during error trials. Warmer colors represent greater activation during correct trials. The underlying anatomical image was averaged across groups. Image displayed in radiological convention. 1 = left inferior frontal gyrus; 2 = left middle frontal gyrus; 3 = bilateral superior frontal gyrus; 4 = bilateral cerebellum; 5 = left superior temporal gyrus; 6 = left inferior frontal gyrus.

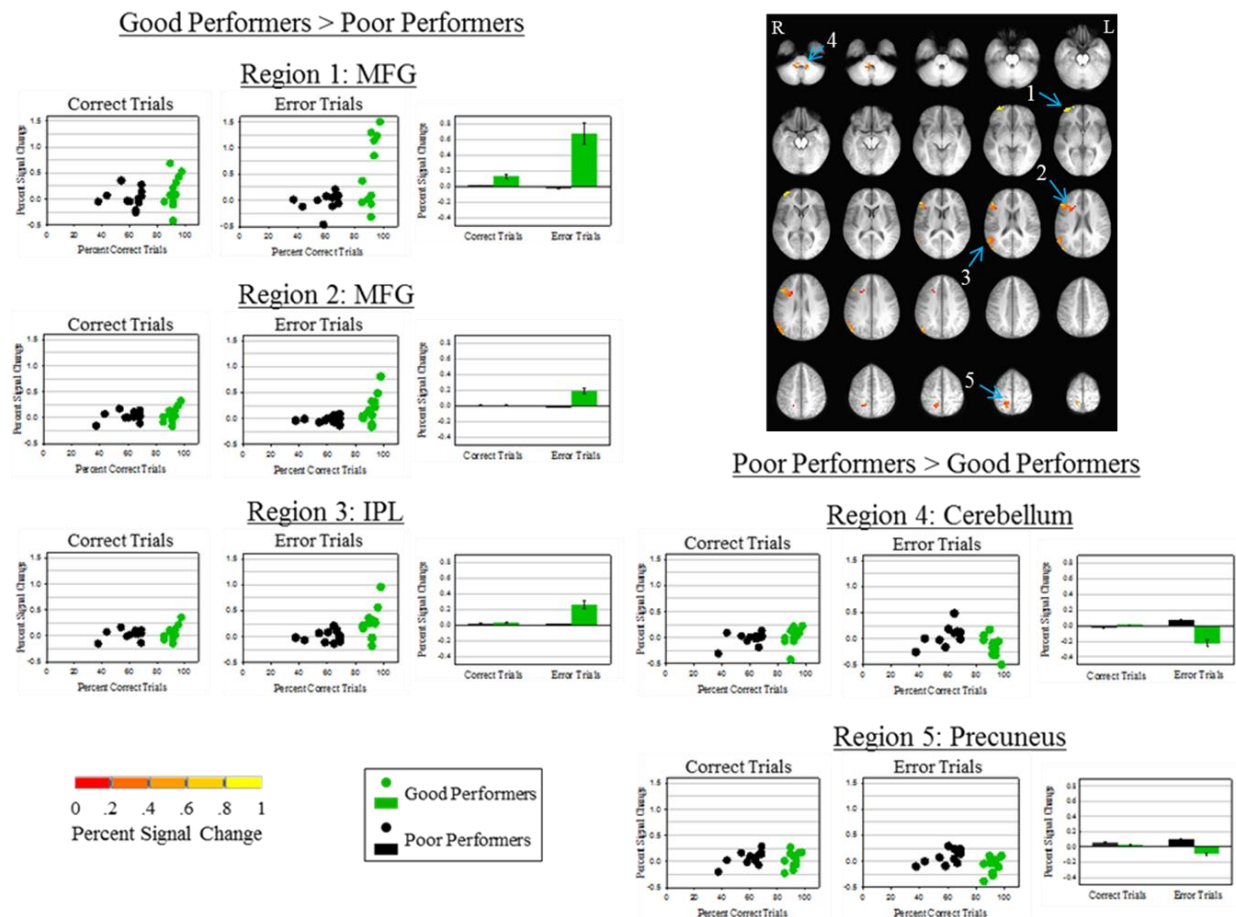


Figure 2.5: Group x Trial Performance interaction. Axial slices ($z = -35$ through $z = 62$, functional slice thickness = 4mm) displaying activation significant at $\alpha = .05$ (corrected) for the group (good and poor performers) by trial performance (correct and error trials) interaction. Scatter plots show percent BOLD signal change values as a function of percent correct trials for individual good and poor performers on correct and error trials. Bar graphs display means and standard error of scatter plots. Regions 1, 2 and 3 showed greater percent BOLD signal change elicited by good performers > than by poor performers on error trials. Regions 4 and 5 showed greater percent BOLD signal change elicited by poor performers than by good performers on error trials. The underlying anatomical image was averaged across groups. Image displayed in radiological convention.

CHAPTER 3

WHITE MATTER STRUCTURAL INTEGRITY DIFFERS BETWEEN PEOPLE WITH
SCHIZOPHRENIA AND HEALTHY GROUPS AS A FUNCTION OF COGNITIVE
CONTROL¹

¹ Schaeffer, D. J., Rodrigue, A. L., Pierce, J. E., Unsworth, N., Clementz, B. A., & McDowell, J.

E. 2015. *Schizophrenia Research*, 169:62-68.

Reprinted here with permission of the publisher.

Abstract

A behavioral hallmark of schizophrenia is poor cognitive control. Recent evidence suggests that problems with cognitive control in schizophrenia are related to disconnectivity along major white matter fibers. Although deficits of cognitive control are common in schizophrenia, a proportion of otherwise healthy subjects show poor cognitive control performance. The present study sought to address this potential confound by comparing white matter integrity between a group with schizophrenia and otherwise healthy individuals with either high or low levels of cognitive control (based on working memory span performance). Diffusion tensor imaging was used to evaluate white matter integrity in 24 participants with schizophrenia, 24 healthy participants with high cognitive control (HCC), and 25 healthy participants with low cognitive control (LCC). To test for differences in fractional anisotropy (FA) across major white matter fiber tracts, a voxelwise region of interest analysis was conducted in standardized brain space. In a separate analysis, regions of interest were manually drawn in native brain space to isolate superior longitudinal fasciculus (SLF), a tract implicated in cognitive control performance. The voxelwise analysis demonstrated widespread lower FA in the schizophrenia group compared to the HCC group. With a high degree of concordance, the manual ROI analysis revealed lower FA in the schizophrenia group compared to the HCC group. Taken together, these results provide evidence to suggest that structural differences identified between healthy groups and schizophrenia may not be entirely specific to the disease process and can vary as a function cognitive control capacity in the comparison group.

Introduction

Schizophrenia is characterized by problems with cognitive control. Recent diffusion tensor imaging (DTI) evidence suggests that deficits in cognitive control in people with schizophrenia are associated with white matter structural deviations across the brain (Liu et al., 2013), particularly in frontal and parietal regions (Karlsgodt et al., 2008). Similar frontal and parietal regions are implicated in poor cognitive control in healthy individuals, with lower cognitive control scores linked to lower structural integrity of fronto-parietal connections (Burzynska et al., 2011). Although deficits of cognitive control are a behavioral hallmark of schizophrenia, some healthy subjects from the general population show poor cognitive control performance and similar deficits in the underlying white matter substrates (Hutton & Ettinger, 2006; Karlsgodt et al., 2008). As such, cognitive control ability may be a mediating factor in typical comparisons between healthy individuals and people with schizophrenia, with variance in structural differences related to cognitive control rather than to the disease process of schizophrenia. The present study sought to test this potential confound by identifying groups of healthy participants with either a high level of cognitive control (HCC) or low level of cognitive control (LCC) based on working memory performance and compare white matter structure across HCC, LCC, and a group of subjects with chronic schizophrenia.

Although the etiologies of schizophrenia have yet to be identified, one theory is that schizophrenia is a disease of disconnectivity (Friston, 1998). DTI is well suited to explore this theory, as it allows for assessment of the relationships between structural disconnectivity and cognitive dysfunction. Present day findings using DTI, however, have provided mixed results as to the white matter structural connections related to schizophrenia symptomatology (see Kubicki et al., 2007 for review). Some authors suggest that discrepancies in white matter findings may

be due to heterogeneity of patient characteristics (Liu et al., 2013) or methodological factors, including inconsistencies in data acquisition, processing, or analysis (Kubicki et al., 2007; Whitford et al., 2011). This drives a need to systematically remove confounds of both participant and methodological variety from DTI analyses of schizophrenia. The present study sought to accomplish this by accounting for the level of cognitive control in the healthy comparison groups through stringent participant matching criteria and by comparing results from multiple DTI analysis types on a single dataset.

Despite inconsistent DTI findings of schizophrenia-specific alterations in white matter, the superior longitudinal fasciculus (SLF; a fronto-parietal tract) has emerged as one of the most reliably identified. Kubicki and Shenton (2009) estimate that SLF is the most consistently identified structure in DTI voxel-based morphometric (VBM) studies, with 33% of the studies reporting schizophrenia-related reductions in SLF integrity. SLF fractional anisotropy (FA; a scalar measure of diffusivity) is reduced in people with schizophrenia as compared to controls (Karlsgodt et al., 2008). Additionally, higher FA values in SLF are correlated with better cognitive control performance in schizophrenia and healthy controls (Karlsgodt et al., 2008). The SLF connects frontal and parietal regions which are structurally and functionally identified as regions mediating cognitive control in healthy samples (Burzynska et al., 2011; Schaeffer et al., 2013). In view of these findings, variability in structural integrity of the SLF likely mediates cognitive control in both schizophrenia and healthy groups.

Based on evidence linking cognitive control and white matter integrity, we sought to test the following hypotheses: (1) That white matter structural integrity (as measured by FA and radial diffusivity (RD)) across the brain would demonstrate the following pattern across groups: for FA, schizophrenia would show lower values than HCC, but not differ from LCC. For RD

(which typically shows an inverse relationship with FA), schizophrenia would show higher values than HCC, but schizophrenia and LCC would not differ. (2) That the SLF, a tract identified as being involved in cognitive control, would differ in FA and RD between HCC and the groups with low cognitive control (LCC and schizophrenia), but not between the schizophrenia and LCC groups, who show more similar cognitive control performance. To test these hypotheses, the present study used two complementary DTI analysis approaches. In the first analysis, voxelwise FA values were compared across major white matter tracts using a region of interest approach. In a second analysis, manual fiber tracing was used to isolate bilateral SLF in DTI native space, with the goal of mitigating the effects of spatial transformation and testing a hypothesis (hypothesis 2 above) specific to the SLF. By using these spatially discrete methods (voxelwise in standard space and fiber tracing in native space), we sought to test if between group differences were robust and not a function of analysis type. In summary, the present study sought to identify schizophrenia-specific alterations in white matter integrity through the use of highly specified control groups (HCC and LCC) and two complementary DTI analyses.

Methods

Participants. Twenty four subjects with schizophrenia were recruited through outpatient centers in Athens and Augusta, GA, USA. For the comparison groups, a large initial sample of healthy people ($N = 235$; mean age = 31.0, $SD = 11.5$; 53% female) was recruited via newspaper ads and flyers posted around Athens, GA, USA to participate in the cognitive control screening session of this study. Based on a distribution of cognitive control performance from this large sample, 24 HCC and 25 LCC participants (age matched to schizophrenia subjects; see Table 3.1 for demographics) returned for DTI acquisition along with the schizophrenia subjects. HCC and

LCC participants had no history of psychiatric illness. All participants were interviewed using the Non-Patient or Patient edition of the Structured Clinical Interview for DSM-IV (First et al., 2002a; First et al., 2002b) and were free from severe head trauma, or current drug or alcohol abuse (via self-report). Participants were screened for contraindications for MRI (e.g., pacemaker or metal in body). Participants provided written informed consent and were compensated \$20 per hour for their participation. The University of Georgia Institutional Review Board approved this study.

Materials and Procedure

Cognitive control screening. Following initial screening, potential participants ($N = 235$) completed three computer-administered complex span tasks (operation span, reading span, and symmetry span; Unsworth et al., 2005; Unsworth and Spillers, 2010) from which a composite score was derived. The operation span task consists of remembering letters while solving unrelated math operations, the reading span task consists of remembering letters while reading unrelated sentences (and making judgments about them), and the symmetry span task requires the recall of spatial sequences of red squares within a matrix while performing a symmetry-judgment task. The score for each task is the number of to-be-remembered items recalled in the correct order. For cognitive control composite scores, each participant's score was z-transformed (based on the means and standard deviations from a previously defined distribution of over 500 participants; Unsworth et al., 2012) and the three z-scores were averaged. This composite score is a broad measure of cognitive control and reduces the probability that task-specific variance is influencing categorization of cognitive control. Only individuals scoring in the upper (HCC, $z \geq 0.57$) and lower (LCC, $z \leq -0.38$) quartiles were asked to participate in the diffusion MRI portion of the study.

Diffusion MRI data acquisition. Images were acquired at the University of Georgia on a 3T GE Signa Excite HDx MRI system (General Electric Medical Systems, Milwaukee, Wisconsin, USA) with an 8 channel head-coil (Model 800152; Invivo Corporation, Gainesville, Florida, USA). During scanning, head positions were stabilized with foam padding. Diffusion images were acquired using an echo planar imaging sequence (acquisition matrix = 128 x 128, 55 interleaved slices, voxel size = 2 x 2 x 2.4 mm, FOV = 256 x 256 mm, TR = 16100 ms, TE = min-full, 3 b = 0 images, 30 diffusion weighted images, $b = 1000 \text{ s/mm}^2$).

Diffusion MRI preprocessing and analysis. Raw diffusion images were converted from GE DICOM format to NIFTI format using the dcm2nii tool (Rorden, 2007). For each subject, volumes were visually inspected for motion artifacts; volumes distorted by motion were removed from the image series and b value/vector tables (1.5% of total volumes removed; average number of volumes/subject removed = 1). Diffusion tensor image analysis was conducted using the FMRIB Software Library (University of Oxford, Oxford, England; Smith et al., 2004). Diffusion images were corrected for eddy-current-induced distortions. Simple head motion was corrected through an affine registration to the first (of three) non-diffusion weighted images ($b = 0$) acquired prior to the diffusion weighted volumes. Nonbrain tissue was removed using the Brain Extraction Tool (Smith, 2002).

Voxelwise regions of interest. FA images were created by fitting diffusion tensors to each voxel using the Diffusion Toolbox. Voxelwise analysis of FA data was carried out using TBSS (Smith et al., 2006). FA images were aligned and transformed into standard space (MNI152; Montreal Neurological Institute, McGill University, Montreal, Quebec, Canada). Individual FA images contributed to a cross-subject mean FA image which was used to generate a FA skeleton representing the center of large fiber tracts common across the group. Whole brain

voxelwise FA values were then constrained using a region of interest analysis, with a series of masks (Figure 3.1) applied to each subject to quantify FA in the “center” of 20 major white matter fiber tracts. First, a mask based on each subject’s FA image was generated to include FA values greater than or equal to 0.2 (Mabbott et al., 2009). Second, the Johns Hopkins University white matter tractography atlas (Hua et al., 2008) was used to create binary masks corresponding to each tract based on probability values (i.e. the probability that a voxel contains the tract); values greater than or equal to 5% were included in the mask (Fjell et al., 2008). Third, a TBSS FA skeleton mask was applied to each individual to include only voxels containing white matter which were common to the group. After applying the masks, mean FA and RD values were calculated for each of the 20 fiber tracts in the tractography atlas. Statistical analyses were conducted in SPSS version 17. One-way ANOVAs were used to test for omnibus effects and independent sample *t* tests for between-group comparisons. In the present study, *both* FA and RD needed to show significant regional variability between groups to qualify as a difference in white matter integrity. FA alone does not capture alterations in white matter integrity as clearly as when RD is considered simultaneously. Although FA is sensitive to microstructural alterations, it does not indicate whether the differences are due to axial or radial diffusivity (Alexander et al., 2008). Relationships between FA or RD values and cognitive control composite scores were assessed with Pearson correlations and corrected for multiple comparisons with permutation testing using MATLAB software version 8.4 (The MathWorks, Inc., Natick, Massachusetts, United States).

Fiber tracking. Tractography was conducted using the ExploreDTI software package (Leemans et al., 2009) with whole brain tensors in DTI native space. A deterministic streamline tractography algorithm (Basser et al., 2000) was used, with a FA threshold of 0.2, an angle

threshold of 45 degrees, and a fiber length minimum of 50 mm. To isolate the SLF, regions of interest were drawn (Figure 3.3) following established anatomical markers (Wakana et al., 2007): First, a coronal slice was selected in the middle of the posterior limb of the internal capsule and a region of interest was drawn around the core of the SLF (identified as a triangular shape, with an anterior-posterior orientation; Wakana et al. 2007). Second, a coronal slice was selected at the middle of the splenium of the corpus callosum, and a region of interest drawn around the anterior-posterior facing fibers. Regions of interest were drawn by two researchers experienced in fiber tracking, who were blind to group assignment and showed a high inter-rater reliability, $\alpha = .98$. Given the high inter-rater reliability, the values from researcher one were chosen for analysis. Average diffusivity values (FA and RD) were extracted for each subject's left and right SLF. One-way ANOVAs were used to test for omnibus effects and independent sample t tests for between-group comparisons.

Results

Cognitive Control Performance. Cognitive control performance significantly differed across groups ($F(2, 64) = 48.32, p = .00$), with the schizophrenia group showing lower cognitive control composite scores (mean = -2.64, SE = .17) than the HCC (mean = .45, SE = .18; $t(40) = 8.63, p = .00$) and LCC (mean = -1.48, SE = .16; $t(46) = 3.38, p = .00$) groups. The HCC group showed higher scores than the LCC group ($t(46) = 8.13, p = .00$). Cognitive control composite scores were positively correlated with FA across groups; similarly, cognitive control composite scores negatively correlated with RD across groups (see Table 3.2 for specific tracts and statistics).

Diffusion MRI

Voxelwise regions of interest. Only tracts with significant FA and RD omnibus effects were tested using specific t contrasts (see Figure 3.2; Table 3.3 for statistics). Schizophrenia showed lower FA and higher RD compared to the HCC group in left anterior thalamic radiation, bilateral inferior frontal-occipital fasciculus, bilateral inferior longitudinal fasciculus, bilateral SLF, and left SLF temporal. SLF temporal and SLF are separate tracts in the Johns Hopkins University atlas, but show a large degree of overlap (i.e., draw from many of the same voxels); SLF temporal accounts for only the inferior portion of SLF and SLF accounts for both inferior and superior portions. LCC did not significantly differ from the schizophrenia or HCC groups in any of the 20 tracts tested.

Fiber tracking. Left SLF showed significant differences in FA ($F(2, 70) = 5.11, p = .00$) and RD ($F(2, 70) = 4.35, p = .01$) across groups (see Figure 3.3). Schizophrenia showed lower FA ($t(46) = 3.04, p = .00$) and higher RD ($t(46) = 2.72, p = .00$) than the HCC group. LCC did not significantly differ in FA or RD between the schizophrenia or HCC groups. Right SLF did not significantly differ across groups in FA ($F(2, 70) = 2.36, p = .10$) or RD ($F(2, 70) = 2.77, p = .06$). FA calculated via the voxelwise region of interest analysis (above) showed a high degree of concordance with the FA values calculated via fiber tracking (see Figure 3.2; $r(144) = .82, p = .00$), suggesting that the between-group differences were robust.

Discussion

The focus of the present study was to test for differences in white matter integrity between subjects with schizophrenia and otherwise healthy individuals with either high (HCC) or low (LCC) levels of cognitive control. A voxelwise analysis demonstrated widespread deficits in white matter between the schizophrenia and HCC groups. In a separate analysis, manual fiber

tracing revealed results concordant with the voxelwise analysis, with the schizophrenia group showing deficits in white matter integrity in SLF when compared to the HCC group. Overall, these results indicate that white matter structural differences between people with schizophrenia and healthy groups vary as a function of cognitive control.

We employed a voxelwise analysis (TBSS) to test for differences in white matter integrity (assessed by FA and RD) across major white matter fiber tracts of the brain. Twenty tracts were included in our analysis, covering all major white matter tracts contained within the Johns Hopkins University white matter tractography atlas (Hua et al., 2008). The analysis revealed widespread differences in FA and RD between the schizophrenia and HCC groups. Of the twenty tracts, eight showed significantly lower FA and higher RD in the schizophrenia group compared to the HCC group, a pattern indicative of less axonal coherence and myelination (Lebel et al., 2008; Song et al., 2002). Widespread reductions in white matter integrity are documented in a number of comparisons between people with schizophrenia and their healthy counterparts (Griffa et al., 2015; Kubicki et al., 2007; Roalf et al., 2015a; Wheeler and Voineskos, 2014). The specific brain regions affected in schizophrenia, however, vary between studies as do the regions correlated with cognitive performance (Kubicki et al., 2007; Wheeler and Voineskos, 2014). These inconsistencies suggest that disruption of white matter in schizophrenia represents a complex constellation of white matter deficits that underlie deficits in neurocognitive performance (Roalf et al., 2015a). Alternatively, such variability could be due to etiological heterogeneity underlying various clinical presentations of schizophrenia. Future studies aimed at identifying heritability of structural alterations in schizophrenia may serve to elucidate etiological variability (Clementz et al., 2015; Roalf et al., 2015b).

Of the twenty tracts, only SLF showed differences in both FA and RD between the LCC group and the HCC group (albeit trend level after familywise error correction). Specifically, the LCC group showed decreased FA and increased RD compared to the HCC group, a pattern indicative of less axonal coherence and myelination (Lebel et al., 2008; Song et al., 2002). Finding lower white matter integrity in the LCC group is consistent with evidence suggesting that white matter integrity of the SLF modulates cognitive control performance (Burzynska et al., 2011). The SLF connects frontal and parietal regions which are functionally implicated as regions mediating cognitive control in healthy samples (Ford et al., 2005; Schaeffer et al., 2013). A recent fMRI-DTI study demonstrated that white matter integrity of SLF is associated with less BOLD responsivity in prefrontal cortex (Burzynska et al., 2011). Because the SLF is bidirectional (sharing efferent fibers to and from cortical regions) in humans, it is likely that prefrontal areas (e.g., dorsolateral prefrontal cortex; DLPFC) send inhibitory signals to parietal cortex via SLF fibers (Makris et al., 2005). Such signals could be hypothesized to modulate top-down control during tasks requiring cognitive control (e.g., antisaccade tasks), with DLPFC and parietal activation linked to response inhibition in saccadic fMRI studies (DeSouza et al., 2003; Ford et al., 2005; Schaeffer et al., 2013). These signals ultimately result in top-down control of superior colliculus via inhibitory signaling (Pierrot-Deseilligny et al., 1991) or, as suggested by more recent evidence, possibly via excitatory signaling (Johnston et al., 2013). Accordingly, reductions in white matter integrity in SLF of the LCC group may account for less efficient transmission of fronto-parietal modulatory signals, resulting in lower cognitive control performance.

Heterogeneity in methodology may also contribute to differences in findings across studies of white matter integrity in schizophrenia. One source of variability is the type of analysis

used, with substantial differences in how structural images are transformed between methods (Wheeler and Voineskos, 2014). In the present study, we aimed to mitigate variability due to the type of spatial transformation by analyzing the DTI images with two complementary analysis methods: one in standard space (TBSS analysis) and the other in native space (i.e., not transformed; fiber tracking analysis). Each analysis has weaknesses, with TBSS subject to partial volume effects and misregistration, and the efficacy of fiber tracking depending on the ability to manually identify white matter structures. Likewise, each analysis has strengths, with TBSS projecting the data onto a white matter skeleton to increase power through dimensionality reduction (Smith et al., 2006) and fiber tracking avoiding misalignment issues altogether through analysis in native space. Despite these differences, our results from these two analysis types yielded highly concordant results ($r = .82$). This high level of concordance suggests that the alterations in SLF in the present study were reliably measured with both methodologies.

A caveat of this study stems from our definition of altered white matter integrity – both FA and RD needed to show significant regional variability between groups to qualify as a difference in white matter integrity. Other canonical DTI studies often use only FA as an index of white matter integrity. Here, if we only considered FA, the results would warrant a different interpretation, with the LCC group showing widespread differences in FA from the HCC group. Simultaneous consideration of FA and RD provides a more veridical and accurate assessment of white matter integrity. Although FA is very sensitive to microstructural alterations, it does not indicate whether the differences are due to axial or radial diffusivity (Alexander et al., 2008). Thus, utilizing the additional diffusion measure of RD in the present study was intended to maximize specificity.

The present findings provide evidence to suggest that structural differences identified between schizophrenia and healthy groups may not be entirely specific to the disease process and can vary as a function of cognitive control capacity in the comparison group. Here, the schizophrenia group showed lower white matter integrity across the brain when compared to a group with high cognitive control, but did not show any structural differences when compared to a group with low cognitive control. These results highlight the use of a behaviorally matched comparison group – future studies might improve the specificity of their results by matching schizophrenia groups to healthy groups with similar levels of cognitive control. Reliably identifying white matter alterations specific to schizophrenia may aid in characterizing phenotypes of schizophrenia (as part of a multivariate biomarker battery; Clementz et al., 2015), which will ultimately lead to a better understanding of the pathophysiology underlying this devastating disorder.

References

- Alexander, A.L., Lee, J.E., Lazar, M., Field, A.S., 2007. Diffusion tensor imaging of the brain. *Neurotherapeutics* 4(3) 316–329.
- Basser, P.J., Pajevic, S., Pierpaoli, C., Duda, J., Aldroubi, A., 2000. In vivo fiber tractography using DT-MRI data. *Magn Reson Med* 44 625-632.
- Burzynska, A.Z., Nagel, I.E., Preuschhof, C., Li, S.C., Lindenberger, U., Bäckman, L., Heekeren, H.R., 2011. Microstructure of frontoparietal connections predicts cortical responsivity and working memory performance. *Cereb. Cortex* 21(10) 2261–71.
- Clementz, B.A., Sweeney, J., Keshavan, M.S., Pearlson, G., Tamminga, C.A., 2015. Using biomarker batteries. *Biol. Psychiatry* 77(2) 90–2.
- Fjell, A.M., Westlye, L.T., Greve, D.N., Fischl, B., Benner, T., van der Kouwe, A.J.W., Salat, D., Bjornerud, A., Due-Tonnessen, P., Walhovd, K.B., 2008. The relationship between diffusion tensor imaging and volumetry as measures of white matter properties. *NeuroImage* 42(4) 1654–68.
- Ford, K.A., Goltz, H.C., Brown, M.R.G., & Everling, S., 2005. Neural processes associated with antisaccade task performance investigated with event-related fMRI. *J. Neurophysiology*. 94(1) 429-40.
- Friston, K.J., 1998. The disconnection hypothesis. *Schizophr. Res.* 30(2) 115–25.
- Griffa, A., Baumann, P.S., Ferrari, C., Do, K.Q., Conus, P., Thiran, J.P., Hagmann, P., 2015. Characterizing the connectome in schizophrenia with diffusion spectrum imaging. *Hum. Brain Mapp.* 36(1) 354–66.

- Hua, K., Zhang, J., Wakana, S., Jiang, H., Li, X., Reich, D.S., Calabresi, P.A., Pekar, J.J., van Zijl, P.C., Mori, S., 2008. Tract probability maps in stereotaxic spaces: Analyses of white matter anatomy and tract-specific quantification. *NeuroImage* 39(1) 336–47.
- Hutton, S.B., & Ettinger, U., 2006. The antisaccade task as a research tool in psychopathology: a critical review. *Psychophysiology* 43 302–313.
- Karlsgodt, K.H., van Erp, T.G.M., Poldrack, R.A., Bearden, C.E., Nuechterlein, K.H., Cannon, T.D., 2008. Diffusion tensor imaging of the superior longitudinal fasciculus and working memory in recent-onset schizophrenia. *Biol. Psychiatry* 63(5) 512–8.
- Kubicki, M., McCarley, R., Westin, C.F., Park, H.J., Maier, S., Kikinis, R., ... Shenton, M.E., 2007. A review of diffusion tensor imaging studies in schizophrenia. *J. Psychiatr. Res.* 41(1-2) 15–30.
- Kubicki, M., Shenton, M.E., 2009. Diffusion MRI in neurological disorders. in: Johansen-Berg, H., Behrens, T.E.J. (Eds.), *Diffusion MRI: From quantitative measurement to in vivo neuroanatomy*. Academic Press. pp. 251–270
- Lebel, C., Walker, L., Leemans, A., Phillips, L., Beaulieu, C., 2008. Microstructural maturation of the human brain from childhood to adulthood. *NeuroImage* 40(3) 1044–55.
- Leemans, A., Jeurissen, B., Sijbers, J., & Jones, D., 2009. ExploreDTI: a graphical toolbox for processing, analyzing, and visualizing diffusion MR data. In Paper presented at the 17th Annual Meeting of Intl Soc Mag Reson Med. Hawaii, U.S.A.
- Liu, X., Lai, Y., Wang, X., Hao, C., Chen, L., Zhou, Z., Yu, X., Hong, N., 2013. Reduced white matter integrity and cognitive deficit in never-medicated chronic schizophrenia: a diffusion tensor study using TBSS. *Behavioural Brain Research* 252 157–63.

- Mabbott, D.J., Rovet, J., Noseworthy, M.D., Smith, M.L., & Rockel, C., 2009. The relations between white matter and declarative memory in older children and adolescents. *Brain Res.* 1294 80–90.
- Roalf, D.R., Gur, R.E., Verma, R., Parker, W.A., Quarmley, M., Ruparel, K., Gur, R.C., 2015a. White matter microstructure in schizophrenia: Associations to neurocognition and clinical symptomatology. *Schizophr. Res.* 161(1) 42–9.
- Roalf, D.R., Vandekar, S.N., Almas, L., Ruparel, K., Satterthwaite, T.D., Elliott, M.A., Podell, J., Gallagher, S., Jackson, C.T., Prasad, K., Wood, J., Pogue-Geile, M.F., Nimgaonkar V.L., Gur, R.E., 2015b. Heritability of subcortical and limbic brain volume and shape in multiplex- multigenerational families with schizophrenia. *Biol. Psychiatry* 77(2) 137–146.
- Rorden, C. 2007. DCM2NII. (Version October 7) [Computer software].
- Schaeffer, D.J., Amlung, M.T., Li, Q., Krafft, C.E., Austin, B.P., Dyckman, K.A., & McDowell, J.E., 2013. Neural correlates of behavioral variation in healthy adults' antisaccade performance. *Psychophysiology* 50(4) 325–33.
- Smith, S.M., 2002. Fast robust automated brain extraction. *Hum. Brain Mapp.* 17(3) 143–55.
- Smith, S.M., Jenkinson, M., Johansen-Berg, H., Rueckert, D., Nichols, T.E., Mackay, C.E., Watkins, K.E., Ciccarelli, O., Cader, M. Z., Matthews, P.M., Behrens, T.E.J., 2006. Tract-based spatial statistics: Voxelwise analysis of multi-subject diffusion data. *NeuroImage* 31(4) 1487–505.
- Smith, S.M., Jenkinson, M., Woolrich, M.W., Beckmann, C.F., Behrens, T.E.J., Johansen-Berg, H., Bannister, P.R., De Luca, M., Drobnjak, I., Flitney, D.E., Niazy, R.K., Saunders, J., Vickers, J., Zhang, Y., Stefano, N.D., Brady, J.M., Matthews, P.M., 2004. Advances in

functional and structural MR image analysis and implementation as FSL. *NeuroImage* 23 S208–19.

Song, S.K., Sun, S.W., Ramsbottom, M.J., Chang, C., Russell, J., Cross, A.H., 2002.

Dysmyelination revealed through MRI as increased radial (but unchanged axial) diffusion of water. *NeuroImage* 17(3) 1429–36.

Unsworth, N., Heitz, R.P., Schrock, J.C., & Engle, R.W., 2005. An automated version of the operation span task. *Behav. Res. Methods* 37(3) 498–505.

Unsworth, N., & Spillers, G.J., 2010. Working memory capacity: Attention control, secondary memory, or both? A direct test of the dual-component model. *J. Mem. Lang.* 62(4) 392–406.

Unsworth, N., Spillers, G.J., Brewer, G.A., 2012. The role of working memory capacity in autobiographical retrieval: individual differences in strategic search. *Memory* 20(2) 167–76.

Wakana, S., Caprihan, A., Panzenboeck, M.M., Fallon, J.H., Perry, M., Gollub, R.L., Hua, K., Zhang, J., Jiang, H., Dubey, P., Blitz, A., van Zijl, P., Mori, S., 2007. Reproducibility of quantitative tractography methods applied to cerebral white matter. *NeuroImage* 36(3) 630–44.

Wheeler, A.L., Voineskos, A.N., 2014. A review of structural neuroimaging in schizophrenia: from connectivity to connectomics. *Front. Hum. Neurosci.* 8 1–18.

Whitford, T.J., Kubicki, M., Shenton, M.E., 2011. Diffusion tensor imaging, structural connectivity, and schizophrenia. *Schizophrenia Research and Treatment* 2011 1-7.

Table 3.1: Participant demographics.

	HCC	LCC	SZ
N	24	25	24
Age (years)	32.6 (13.6)	32.6 (10.3)	38.5 (9.1)
Gender (N female)	6	18	13
Handedness (N right, left, ambidextrous)	21, 2, 1	20, 5, 0	19, 3, 2
Anti-psychotic (atypical, typical, both; N on)	0, 0, 0	0, 0, 0	14, 3, 1
Anti-cholinergics (N on)	0	0	1
Anti-depressants (N on)	0	0	5
Anti-anxiety (N on)	1	0	3

Patient medication: 18 anti-psychotics only, 1 anti-psychotics and anti-cholinergics, 3 on anti-psychotics and anti-depressants, 2 anti-depressants only, and 3 anti-psychotics and anti-anxiety.

Table 3.2: Pearson correlations between voxelwise ROI tracts and CC composite scores.

Tract	Hemisphere	Measure of diffusivity	<i>r</i> (<i>df</i>)			
			Across groups (HCC, LCC & SZ)	HCC	LCC	SZ
Superior longitudinal fasciculus	L	FA	.44 (66)*	.09 (22)	-.13 (23)	.46 (17)
		RD	-.34 (66)	.27 (22)	-.05 (23)	-.26 (17)
Superior longitudinal fasciculus temporal	L	FA	.45 (66)*	-.03 (22)	-.19 (23)	.45 (17)
		RD	-.32 (66)	.29 (22)	.02 (23)	-.27 (17)
Anterior thalamic radiation	R	FA	.41 (66)*	.04 (22)	.10 (23)	.60 (17)*
		RD	-.37 (66)*	.10 (22)	-.10 (23)	-.43 (17)
Inferior fronto-occipital fasciculus	L	FA	.48 (66)*	-.02 (22)	.06 (23)	.60 (17)*
		RD	-.40 (66)*	.25 (22)	-.10 (23)	-.37 (17)
	R	FA	.40 (66)*	.30 (22)	.07 (23)	.49 (17)
		RD	-.36 (66)	-.06 (22)	-.16 (23)	-.37 (17)
Inferior longitudinal fasciculus	L	FA	.41 (66)*	.29 (22)	.06 (23)	.40 (17)
		RD	-.30 (66)	.00 (22)	-.19 (23)	-.26 (17)
Inferior longitudinal fasciculus	R	FA	.36 (66)*	.18 (22)	.10 (23)	.32 (17)
		RD	-.33 (66)	.10 (22)	-.25 (23)	-.15 (17)
Forceps minor	-	FA	.41 (66)*	.27 (22)	.04 (23)	.55 (17)
		RD	-.18 (66)	-.08 (22)	-.07 (23)	-.34 (17)
Uncinate fasciculus	L	FA	.38 (66)*	.18 (22)	-.05 (23)	.58 (17)
		RD	-.28 (66)	.01 (22)	-.06 (23)	-.42 (17)

Correlations corrected for multiple comparisons via permutation testing.

* Significant correlations.

Table 3.3: Voxelwise ROI fiber tracts with significant F statistics

Tract (HCC > SZ)	Hemisphere	Measure of diffusivity	F (df)	p	M (SD)		t (df)	p FWE
					HCC	SZ		
Superior longitudinal fasciculus	R	FA	4.15 (2, 70)	0.02	0.44 (.01)	0.43 (.02)	2.66 (46)	0.02
		RD	4.35 (2, 70)	0.02	5.71 (.22)	5.92 (.33)	-2.62 (46)	0.01
	L	FA	6.68 (2, 70)	0.00	0.45 (.02)	0.43 (.02)	3.33 (46)	0.00
		RD	5.72 (2, 70)	0.01	5.69 (.21)	5.93 (.33)	-3.00 (46)	0.00
Superior longitudinal fasciculus temporal	L	FA	8.11 (2, 70)	0.00	0.48 (.02)	0.46 (.03)	3.70 (46)	0.00
		RD	5.30 (2, 70)	0.01	5.47 (.21)	5.70 (.34)	-2.91 (46)	0.01
Anterior thalamic radiation	L	FA	3.30 (2, 70)	0.04	0.46 (.01)	0.45 (.02)	2.21 (46)	0.05
		RD	5.03 (2, 70)	0.01	6.09 (.25)	6.37 (.39)	-2.91 (46)	0.01
Inferior fronto-occipital fasciculus	R	FA	3.71 (2, 70)	0.03	0.49 (.02)	0.48 (.02)	2.50 (46)	0.02
		RD	3.38 (2, 70)	0.04	5.64 (.26)	5.84 (.34)	-2.30 (46)	0.03
	L	FA	5.09 (2, 70)	0.01	0.49 (.02)	0.47 (.03)	2.95 (46)	0.01
		RD	3.82 (2, 70)	0.03	5.68 (.24)	5.90 (.36)	-2.47 (46)	0.02
Inferior longitudinal fasciculus	R	FA	5.21 (2, 70)	0.01	0.47 (.02)	0.45 (.02)	3.23 (46)	0.01
		RD	4.57 (2, 70)	0.01	5.77 (.24)	6.00 (.34)	-2.73 (46)	0.01
	L	FA	8.13 (2, 70)	0.00	0.47 (.02)	0.45 (.02)	3.88 (46)	0.00
		RD	4.92 (2, 70)	0.01	5.83 (.24)	6.08 (.38)	-2.67 (46)	0.01

Individual group contrasts were corrected for multiple comparisons using the Tukey HSD test ($\alpha = 0.05$). Radial diffusivity values are multiplied by 10,000. The following tracts were compared, but not displayed in the table (no significant omnibus effects for FA and RD were found): right anterior thalamic radiation, right and left cingulum (cingulate gyrus), right and left cingulum (hippocampus), right and left corticospinal tract, forceps major and minor, right superior longitudinal fasciculus temporal, and right and left uncinate fasciculus.

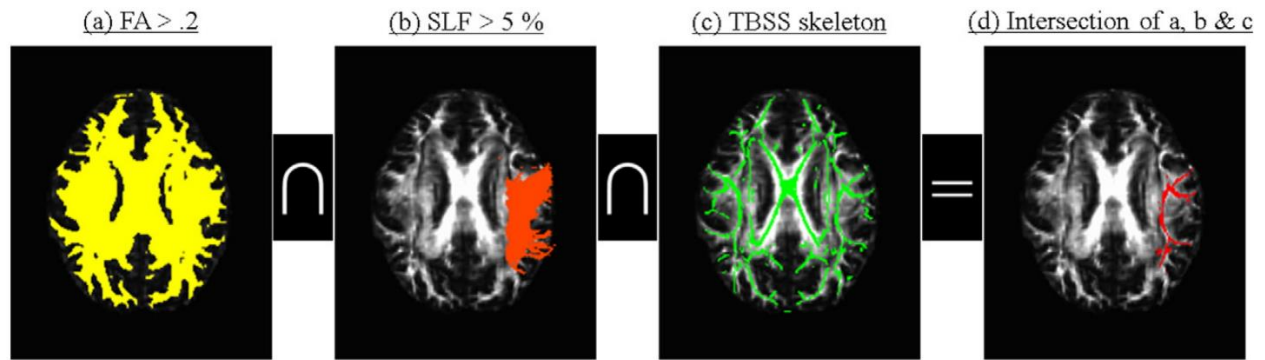


Figure 3.1: Voxelwise region of interest analysis and results. Binary masks overlaid on an axial slice of FA values (mean of entire sample) in MNI space, displayed in radiological convention. Overlay is colored in yellow, orange, or green, indicating which voxels to include in the final analysis (i.e., colored voxels = 1, non-colored voxels = 0; SLF is used as example here). Red voxels (right) shows the intersection the three binary masks ($a \cap b \cap c = d$). Voxels in this resultant mask contributed to a mean for the group comparisons of FA and RD.

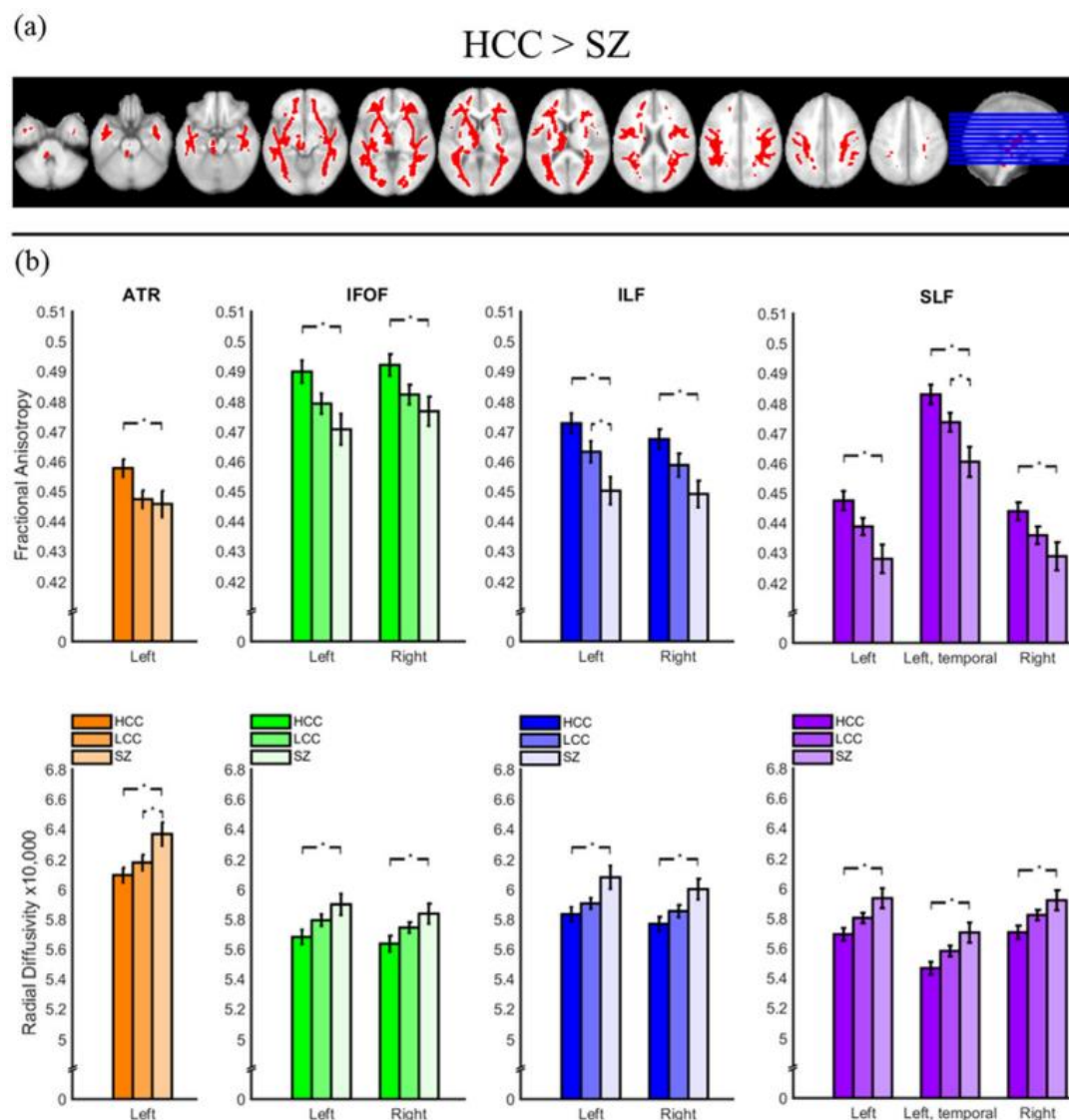


Figure 3.2: Voxelwise region of interest results. (a) Shows a spatial map of the t contrast between HCC and schizophrenia. Red regions illustrate where HCC showed higher FA and lower RD than the schizophrenia group. Regions are thickened to aid in visualization. Significant regions are overlaid on the MNI152 brain, with axial slices $z = -34$ through $z = 46$ displayed (slice spacing = 8 mm). Images displayed in neurological convention. (b) Mean (SE) FA and RD values for regions with significant F values across groups (significant t tests indicated by bar with *). ATR = anterior thalamic radiation; IFOF = inferior fronto-occipital fasciculus; ILF = inferior longitudinal fasciculus; SLF = superior longitudinal fasciculus.

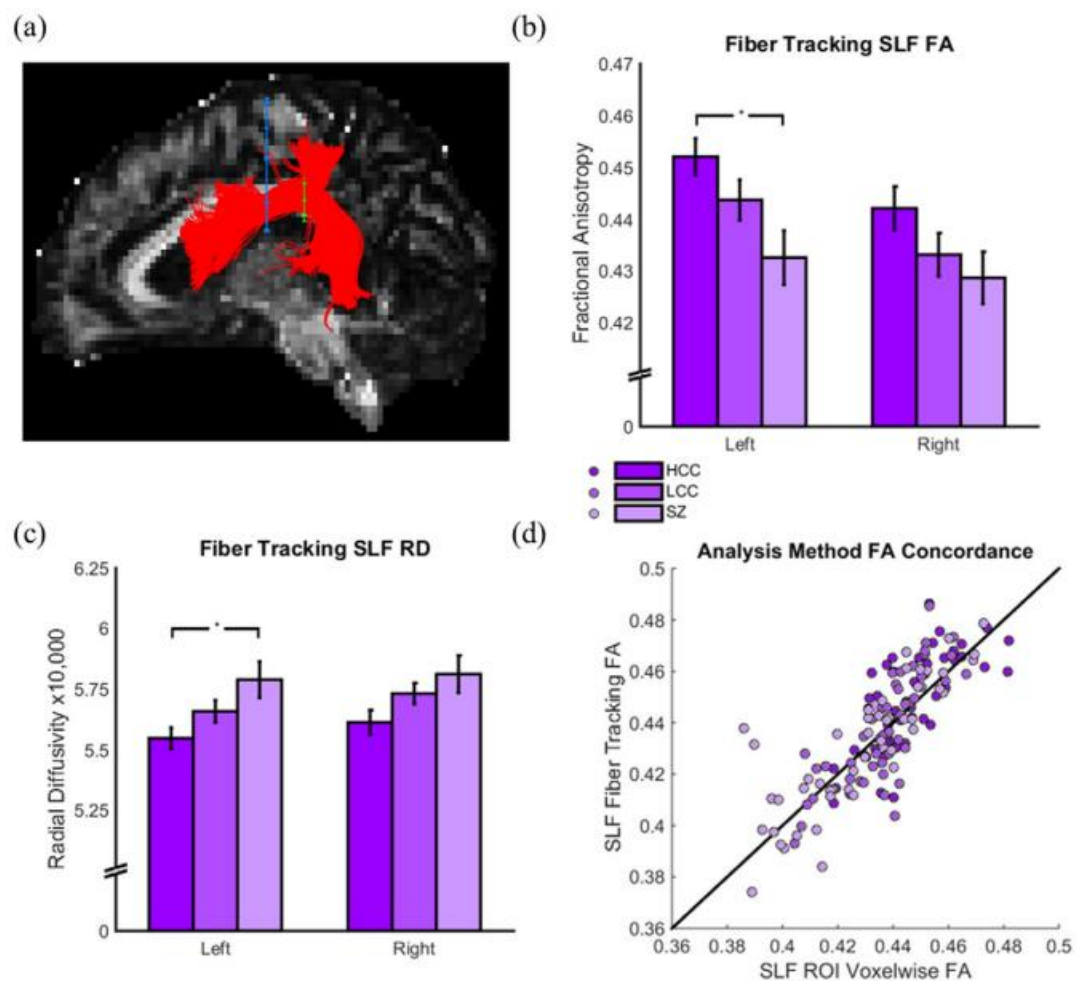


Figure 3.3: Fibers of the SLF from a representative subject. (a) SLF fibers (red) were traced as per Wakana et al. (2007), with the regions of interest shown in blue and green. The underlying map shows an FA map from a representative subject. (b & c) Mean (SE) FA (b) and RD (c) values from fiber tracking left and right SLF. The schizophrenia group showed lower FA and higher RD than the HCC group in left SLF (significant t tests indicated by bar with *). The HCC and LCC did not differ in left or right SLF FA or RD, nor did LCC and schizophrenia. (d) Mean FA values of bilateral SLF for two different analysis methods: voxelwise (x axis) and manual fiber tracing (y axis). The black line indicates the point of exact concordance (45 degrees from the origin). The two methods showed a strong correlation, $r(144) = .82$, $p = .00$.

CHAPTER 4

WHITE MATTER FIBER INTEGRITY OF THE SACCADIC EYE MOVEMENT NETWORK
DIFFERS BETWEEN SCHIZOPHRENIA AND HEALTHY GROUPS¹

¹ Schaeffer, D. J., Rodrigue, A. L., Pierce, J. E., Murphy, M., Clementz, B. A., McDowell, J. E.

Submitted to *Biological Psychiatry*, 03/26/2016.

Abstract

Recent diffusion tensor imaging (DTI) studies suggest that altered white matter fiber integrity is a pathophysiological feature of schizophrenia. Lower white matter integrity is associated with poor cognitive control, a cognitive deficit that is characteristic of schizophrenia and often measured using the antisaccade task. Although the functional neural correlates of poor antisaccade performance have been well studied, fewer studies have investigated the extent to which white matter fibers connecting the functional nodes of the antisaccade network contribute to antisaccade performance. The aim of the present study was to assess the white matter structural integrity of fibers connecting two functional nodes of the saccadic eye movement network implicated in poor antisaccade performance in schizophrenia – putamen of the basal ganglia and medial frontal eye fields (FEF). To evaluate white matter integrity, DTI was acquired on 31 subjects with schizophrenia and 30 behaviorally matched healthy comparison subjects with low levels of cognitive control (LCC group). A second healthy control group of 30 subjects with high levels of cognitive control (HCC group) was also used. White matter fibers were tracked between functional regions of interest (putamen and medial FEF) generated from antisaccade fMRI activation maps (from a previous study) and measures of diffusivity were quantified. The results demonstrated lower white matter integrity (as marked by higher MD and RD) in the schizophrenia group than in the HCC group, but not the LCC group who showed similarly poor cognitive control performance. Overall, the results suggest that these alterations are not specific to the disease process of schizophrenia, but rather a function of decreased cognitive control capacity that is concomitant with the disease.

Introduction

The disconnection hypothesis of schizophrenia posits that dysfunctional integration of neuronal systems is a pathophysiological marker of schizophrenia (1). Diffusion tensor imaging (DTI) studies have yielded support for this theory, revealing alterations in white matter fibers that transmit neural signals across the brain. These alterations are generally characterized by lower fractional anisotropy (FA) and are linked to symptomatology and cognitive dysfunction in schizophrenia (see 2 for review). Reports of the specific fiber bundles related to behavioral dysfunction in schizophrenia, however, have implicated a diverse range of tracts. A potential method for honing in on tracts that are related to behavioral deficits in schizophrenia is to consider altered white matter integrity in the context of a well-studied circuitry that has long been reported to show dysfunction in schizophrenia. The saccadic eye movement system is ideally suited for this task, as a series of studies have reliably demonstrated alterations of saccadic circuitry that relate to poor cognitive control – a hallmark cognitive deficit in schizophrenia (see 3 for review). Differences in antisaccade circuitry in schizophrenia are widely reported in the context of functional magnetic resonance imaging (fMRI), but fewer studies have investigated the extent to which white matter fibers connecting the functional nodes of the antisaccade network contribute to poor antisaccade performance in schizophrenia. This study sought to test for white matter integrity deficits underlying poor antisaccade performance in schizophrenia by leveraging data from two complementary MRI acquisition sequences, DTI and fMRI.

Human neuroimaging studies and non-human primate models of the saccadic eye movement network have elucidated the white matter tracts supporting saccadic performance. A recent integrated DTI and fMRI study explored fibers related to an antisaccade task in a healthy

human sample (4). In this study, the authors tracked fibers seeded in caudate nucleus or putamen of the basal ganglia (manually segmented from T1 weighted images) to the medial FEF, lateral FEF, or supplementary eye fields, which were drawn from fMRI patterns of activation associated with an antisaccade task. The results revealed a greater number of subjects with ipsilateral fiber connections between putamen and the FEF than between caudate nucleus and the FEF. Other DTI evidence suggests that the human premotor cortex, which is directly anterior to FEF, shows a greater degree of connectivity to putamen than caudate nucleus (5). It should be noted that these results differ from non-human primate tracing studies, which indicate clear connections between caudate nucleus and the FEF and less clear labelling in putamen (6, 7). Here, we sought to replicate fiber tracing between putamen and the FEF (as shown in 4) in our healthy sample, and extend these findings by applying this methodology to a sample with schizophrenia.

Selecting fibers that send information to and from basal ganglia is of interest because striatum shows altered BOLD signal during volitional saccadic tasks in schizophrenia samples (8, 9, 10). Morphologically, caudate and putamen also show structural differences in schizophrenia; these differences are modulated by typical and atypical neuroleptics, with related volume increases or decreases, respectively (11). Non-human primate data suggests that the basal ganglia has parallel excitatory and inhibitory loops which preset the motor system to generate a saccade (12); these loops are fed by cortical regions and the resultant signals are output to superior colliculus and thalamus. In schizophrenia, alterations in these loops are related to poor cognitive control performance (13). Specifically, abnormal phasic dopamine release in basal ganglia in schizophrenia may result in abnormal gating of frontal cortical regions (e.g., frontal eye fields) during the execution of motor action plans (e.g., saccadic eye

movements; 14). These studies demonstrate that both structural and functional alterations of basal ganglia are related to cognitive control dysfunction in schizophrenia.

Fibers connecting FEF are implicated in poor antisaccade performance in schizophrenia. Manoach et al. (15) found that decreased FA in white matter underlying FEF was associated with longer saccadic latency in schizophrenia. These findings are congruent with fMRI data which suggests that BOLD signals in the FEF are abnormally delayed and prolonged in schizophrenia (16). Data from healthy samples suggests that timing of FEF activation is crucial for successful performance on antisaccade tasks, with greater pre-stimulus BOLD activation in FEF correlated with faster saccadic triggering (17). Electroencephalography evidence demonstrates a similar effect, with prefrontally distributed pre-stimulus alpha phase effects (likely originating in FEF) linked to saccadic reaction time (18, 19). Given that the interaction of basal ganglia and FEF supports fast and correct saccadic performance in healthy samples, we explored whether the fibers connecting these regions showed alterations in schizophrenia.

As demonstrated by our recent study (20), findings of altered white matter integrity in schizophrenia vary as a function of the cognitive control capacity in healthy comparison groups. Specifically, widespread white matter differences were found between a schizophrenia sample and a healthy comparison group with high levels of cognitive control, but no white matter differences were found between the schizophrenia sample and a behaviorally-matched healthy comparison group with low cognitive control. In light of these findings, the present study consisted of a group with schizophrenia, a healthy group with high cognitive control (HCC), and a healthy group with low cognitive control (LCC). Explicitly, the present study includes an expanded sample from Schaeffer et al. (20). Through stringent participant matching criteria between schizophrenia and comparison groups, we sought to differentiate white matter structural

deficits in schizophrenia that are a function of cognitive control capacity versus those that are specific to the disease process of schizophrenia.

By quantifying the integrity of white matter fibers connecting two functional nodes of the saccadic eye movement network, this study sought to link two lines of evidence in which people with schizophrenia show: (1) lower white matter integrity and (2) poor cognitive control capacity as measured by antisaccade tasks. Specifically, we hypothesized that people with schizophrenia would show lower white matter integrity in fibers which are known to support correct antisaccade performance (those between putamen and medial FEF) as compared to the HCC group, but not the LCC group. To test this hypothesis, fMRI antisaccade data from a previous study (21) was combined with DTI data from the present study. Fibers connecting putamen and medial FEF were then tracked and values of diffusivity compared between schizophrenia, HCC, and LCC groups. In summary, this study aimed to test for altered white matter integrity in a specific subset of fibers connecting a well-documented functional circuitry that is abnormal in schizophrenia.

Method

Participants. Thirty one subjects with schizophrenia were recruited through outpatient centers in Athens and Augusta, GA, USA. For the comparison groups, a large initial sample of healthy people ($N = 235$; mean age = 31.0, $SD = 11.5$; 53% female) was recruited via newspaper ads and flyers posted around Athens, GA, USA to participate in the cognitive control screening session of this study. Based on a distribution of cognitive control performance from this large sample, 30 HCC and 30 LCC participants (age matched to schizophrenia subjects; see Table 4.1 for demographics) returned for DTI acquisition along with 31 schizophrenia subjects. HCC and LCC participants had no history of psychiatric illness. All participants were interviewed using

the Non-Patient or Patient edition of the Structured Clinical Interview for DSM-IV (First et al., 2002a; First et al., 2002b) and were free from severe head trauma, or current drug or alcohol abuse (via self-report). Participants were screened for contraindications for MRI (e.g., pacemaker or metal in body). Participants provided written informed consent and were compensated \$20 per hour for their participation. The University of Georgia Institutional Review Board approved this study.

Materials and Procedure

Cognitive control screening. As described in Schaeffer et al. (20) a large group of people ($N = 235$) was screened using complex span computer tasks (operation span, reading span, and symmetry span; 24, 25) designed to index cognitive control. The score for each task is the number of to-be-remembered items recalled in the correct order. For cognitive control composite scores, each participant's score was z-transformed (based on the means and standard deviations from a previously defined distribution of over 500 participants; 26) and the three z-scores were averaged. This composite score is a broad measure of cognitive control and reduces the probability that task-specific variance is influencing categorization of cognitive control. Only individuals scoring in the upper (HCC, $z \geq 0.57$) and lower (LCC, $z \leq -0.38$) quartiles were asked to participate in the diffusion MRI portion of the study.

Diffusion MRI data acquisition. Images were acquired at the University of Georgia on a 3T GE Signa Excite HDx MRI system (General Electric Medical Systems, Milwaukee, Wisconsin, USA) with an 8 channel head-coil (Model 800152; Invivo Corporation, Gainesville, Florida, USA). During scanning, head positions were stabilized with foam padding. Diffusion images were acquired using an echo planar imaging sequence (acquisition matrix = 128 x 128,

55 interleaved slices, voxel size = 2 x 2 x 2.4 mm, FOV = 256 x 256 mm, TR = 16100 ms, TE = min-full, 3 b = 0 images, 30 diffusion weighted images, $b = 1000 \text{ s/mm}^2$).

Diffusion MRI preprocessing and analysis. Raw diffusion images were converted from GE DICOM format to NIFTI format using the dcm2nii tool (27). For each subject, volumes were visually inspected for motion artifacts; volumes distorted by motion were removed from the image series and b value/vector tables (2.5% of total volumes removed; average number of volumes/subject removed = 1). Diffusion tensor image analysis was conducted using the FMRIB Software Library (University of Oxford, Oxford, England; 30). Diffusion images were corrected for eddy-current-induced distortions. Simple head motion was corrected through an affine registration to the first (of three) non-diffusion weighted images ($b = 0$) acquired prior to the diffusion weighted volumes. Non-brain tissue was removed using the Brain Extraction Tool (28).

Registration of fMRI Regions of Interest to DTI native space. Fibers were tracked between two fMRI regions of interest: putamen of the basal ganglia and the medial FEF. These fMRI based regions of interest were drawn from an fMRI dataset previously collected by our laboratory (see 21 for details). In that sample, fMRI patterns of activation from a block-design antisaccade paradigm were compared between a healthy group with high cognitive control and a separate healthy group with low cognitive control (as measured by antisaccade performance). As these groups were similar to the healthy comparison groups in the present sample (i.e., HCC and LCC) and the two groups showed spatially similar peak activations in putamen and medial FEF, we generated regions of interest based on peak BOLD signal from a t contrast map (i.e., both groups' BOLD activation versus baseline). Specifically, we generated spherical regions of interest in Talaraich space (29) with an 8 mm radius (made large to reach voxels containing

white matter) around the voxel with peak activation in left (Talairach x, y, z coordinates: 25, 5, 12) and right (-22, 1, 12) putamen and left (26, 7, 53) and right (-24, 4, 52) medial frontal eye fields (see Figure 4.1 for visualization). These regions of interest were then spatially transformed from standard space (Talairach space; 29) to DTI native space for each subject in the present sample using the following procedure: First, the Talairach space anatomical image was transformed into DTI native space for each individual (i.e., 91 separate transformations) with a 12 degree of freedom global affine transformation using FSL's FLIRT tool (30). Second, the transformation matrix from this process was stored for each individual. Third, the functional regions of interest (i.e., putamen and medial FEF) were registered into DTI native space by applying previously mentioned transformation matrix.

Fiber tracking. Once the functional seeds were transformed into DTI native space, tractography was conducted using the ExploreDTI software package (31) with whole brain tensors in DTI native space. A deterministic streamline tractography algorithm (32) was used to trace fibers that were seeded in putamen *and* (using “and” Boolean operator) traversed ipsilateral medial FEF, with a FA threshold of 0.2, an angle threshold of 45 degrees, and a fiber length minimum of 50 mm. Because fiber tracking was performed on an individual basis, the fiber patterns from each subject were slightly different; extraneous fibers were removed from analysis using the “not” operator. To index white matter integrity, mean FA, mean diffusivity (MD), axial diffusivity (AD) and radial diffusivity (RD) values were extracted from each subject's fiber pattern (i.e., mean across all isolated fibers for that subject). FA is a scalar measure from 0-1 that ostensibly reflects the degree of myelination and axonal coherence of fiber, with 1 indicating fuller myelination or coherence. In a tensor model, from which FA is derived, three orthogonal Eigen values quantify the magnitude of diffusion (i.e., λ_1 , λ_2 , & λ_3) within a voxel. MD is the

mean of these values and generally has a negative relationship with FA. AD is the value of λ_1 and represents the magnitude of diffusion parallel to axons within that voxel (i.e., along the principle Eigen vector). RD is the mean of λ_2 and λ_3 and represents the magnitude of diffusion perpendicular to axons within a voxel and general has a negative relationship with FA. Group-wise ANOVAs were conducted to isolate omnibus differences in diffusivity. To determine specific group-wise differences, independent sample t tests were conducted.

Results

Cognitive control performance. Cognitive control performance was measured in each group using complex span tasks (24; 25) and a composite z-score was derived. Composite scores significantly differed across groups ($F(2,89) = 67.86, p = .00$), with the schizophrenia group showing lower scores (mean = -2.66, SE = .25) than the HCC (mean = .42, SE = .14; $t(59) = 10.93, p = .00$) and LCC (mean = -1.58, SE = .17; $t(59) = 3.60, p = .00$) groups. The HCC group showed higher scores than the LCC group ($t(58) = 9.04, p = .00$). Cognitive control composite (“SPAN”) scores were negatively correlated with MD and RD of left lateralized fibers when all of the groups were considered together (i.e., across groups; see Figure 4.2 for statistics).

Fiber tracking. Ipsilateral fibers were tracked between putamen and medial FEF in left and right hemispheres for each subject, with mean diffusivity values (FA, MD, AD, RD) output for each tract. Left hemisphere tracts showed significant omnibus effects (see Figure 4.3) in MD ($F(2, 88) = 6.54, p = .00$), AD ($F(2, 88) = 4.22, p = .01$), and RD ($F(2, 88) = 5.22, p = .00$). Right hemisphere tracts showed significant omnibus effects in MD ($F(2, 88) = 3.21, p = .04$) and RD ($F(2, 88) = 3.90, p = .02$) across groups. For MD, schizophrenia showed higher values in left ($t(59) = 13.12, p = .00$) and right ($t(59) = 2.16, p = .03$) hemispheres than the HCC group, but did not differ from the LCC group. For AD, schizophrenia showed higher values in left ($t(59) =$

2.59, $p = .01$) hemisphere than the HCC group, but did not differ from the LCC group. For RD, schizophrenia showed higher values in left ($t(59) = 2.79$, $p = .00$) and right ($t(59) = 2.32$, $p = .02$) hemispheres than the HCC group, but did not differ from the LCC group.

Discussion

This study sought to test for schizophrenia-specific alterations in white matter connections of the saccadic eye movement circuitry by leveraging information from two MRI modalities (fMRI and DTI). White matter fibers were tracked between basal ganglia and the FEF through the use of regions of interest created from fMRI patterns of activation elicited with an antisaccade task (21). These fibers were compared between schizophrenia subjects and two healthy comparison groups with either high (HCC) or low (LCC) levels of cognitive control. The results demonstrated lower white matter integrity (as marked by lower FA (albeit not significant) and higher bilateral MD and RD) in the schizophrenia group than in the HCC group, but not the LCC group who showed similarly poor cognitive control performance. Overall, the results suggest that these alterations are not specific to the disease process of schizophrenia, but rather associated with decreased cognitive control capacity that is frequently concomitant with the disease, but also found sometimes in healthy people.

By integrating a previous fMRI dataset (21) with the current DTI data, we aimed to replicate existing reports of fiber tracking between putamen and the FEF (as shown in 4) in our healthy sample, and extend these findings by applying this methodology to a sample with schizophrenia. Similar to Neggers et al. (4), our results demonstrated white matter fiber connections between putamen and medial FEF in both healthy and schizophrenia samples. Other DTI data in humans (using seed-based connectivity) shows that the putamen has extensive ipsilateral connections across cortex including prefrontal cortex, primary motor area, primary

somatosensory area, supplementary motor area, and premotor area (33). Although DTI does not delineate between anterograde and retrograde connections, these fibers are ostensibly part of reciprocal loops between putamen and cortical areas (in this case, medial FEF). In the context of saccadic eye movements, these loops likely play a role in cognitive control by presetting the saccadic system to perform antisaccades task correctly – i.e. inhibiting a reflexive saccade and executing a volitional saccade away from the cue to an unmarked location in space (4, 9).

Although we do not present antisaccade performance data here directly, low span task scores are related to poor antisaccade performance (34) and thus serve as a proxy for measuring poor cognitive control in schizophrenia. Our results demonstrate that: 1) MD and RD are significantly higher in schizophrenia than in a healthy group with higher cognitive control capacity (HCC group) and 2) higher MD and RD of fibers connecting putamen and medial FEF is related to lower cognitive control performance (i.e., lower SPAN composite scores). Higher MD and RD are indicative of lower axonal coherence or myelination (35, 36); this pattern is typically accompanied by lower FA (not present in this sample, albeit the trend is visible in Figure 4.3). Taken together these results suggest that lower integrity of these fibers, at least in part, accounts for poor cognitive control performance in schizophrenia.

A potential caveat of this study stems from diminished signal quality in basal ganglia. Voxels in sub-cortical regions are more susceptible to magnetic artifact than those in cortex (due to magnetic inhomogeneity around vasculature or sinuses; 37). Additionally, because regions of basal ganglia are highly connected to cortical regions (33), fiber direction assignment becomes difficult when these fibers “kiss” or actually cross, making fiber tract reconstruction difficult. As such, our ability to resolve fibers in close proximity to basal ganglia was likely limited. Future studies may ameliorate this challenge through the use of diffusion spectrum imaging (i.e.,

hundreds of diffusion encoding directions) and by using models which account for multiple fiber direction assignments within a single voxel. Despite this, our results replicated those found with a previous human sample (4) and reflect similar patterns found in non-human primates (6, 7).

Dysfunction of basal ganglia has long been implicated in schizophrenia. Specifically in the context of the volitional saccade tasks, samples with schizophrenia show deficits in activation (as measured by fMRI) in basal ganglia during antisaccade tasks (8, 9, 10). Non-human primate data suggests that caudate and putamen neurons are involved with suppression of inappropriate saccades toward the cue during antisaccade tasks via the indirect pathway, and that pre-stimulus activity in these regions is related to volitional saccades away from the cue (38). Because this feedback loop (i.e., the indirect pathway) receives input from the FEF (39), it is possible that lower white matter integrity of the fibers carrying these input signals could disrupt efficient functioning of this circuitry. Future studies probing this circuitry in schizophrenia samples could provide insight by testing the relationship between white matter fiber integrity and the timing or magnitude of functional activation during an antisaccade task.

In summary, the present results provide evidence that white matter integrity of fibers connecting putamen and FEF are altered in schizophrenia when compared to a group with high cognitive control, but not when compared to a group with low cognitive control. These findings suggest that the alterations are not specific to the disease process of schizophrenia, but rather a function of decreased cognitive control capacity that is concomitant with the disease. These results have implications for the selection of behaviorally matched comparison groups in studies of schizophrenia – future studies may reduce confounding variance in their results by pairing schizophrenia samples with healthy samples that show similarly poor cognitive control performance. Ultimately, understanding how functional and structural substrates interact will

lead to a better understanding of the neural substrates of cognitive control performance in both healthy and diseased states.

References

1. Friston KJ. (1998): The disconnection hypothesis. *Schizophr Res* 30 (2): 115–125.
2. Kubicki M, McCarley R, Westin CF, Park HJ, Maier S, Kikinis R, *et al.* (2007): A review of diffusion tensor imaging studies in schizophrenia. *J Psychiatr Res* 41 (1–2): 15–30.
3. Hutton SB and Ettinger U. (2006): The antisaccade task as a research tool in psychopathology: a critical review. *Psychophysiology* 43: 302–313.
4. Neggers SFW, van Diepen RM, Zandbelt BB, Vink M, Mandl RCW, and Gutteling TP. (2012): A functional and structural investigation of the human fronto-basal volitional saccade network. *PloS One* 7: e29517.
5. Draganski B, Kherif F, Klöppel S, Cook PA, Alexander DC, Parker GJM., *et al.* (2008): Evidence for segregated and integrative connectivity patterns in the human basal ganglia. *J Neuroscience* 28: 7143–7152.
6. Kunzle H and Akert K.(1977): Efferent connections of cortical, area 8 (frontal eye field) in macaca fascicularis. A reinvestigation using autoradiographic technique. *J Comp Neurol* 173 (1): 147-164.
7. Astruc, J. (1971): Corticofugal connections of area 8 (frontal eye field) in macaca mulatta. *Brain Res* 33: 241-256.
8. Camchong J, Dyckman KA, Chapman CE, Yanasak NE, and McDowell JE. (2006): Basal ganglia-thalamocortical circuitry disruptions in schizophrenia during delayed response tasks. *Biol Psychiat* 60: 235–241.
9. Raemaekers M, Jansma JM, Cahn W, Van der Geest JN, van der Linden JA, Kahn RS, *et al.* (2002): Neuronal substrate of the saccadic inhibition deficit in schizophrenia investigated

- with 3-dimensional event-related functional magnetic resonance imaging. *Arch Gen Psychiat* 59: 313-320.
10. Tu P, Buckner RL, Zollei L, Dyckman KA, Goff DC, and Manoach DS. (2010): Reduced functional connectivity in a right-hemisphere network for volitional ocular motor control in schizophrenia. *Brain* 133: 625–637.
 11. Corson PW, Nopoulos P, Miller DD, Arndt S, and Andreasen NC. (1999): Change in basal ganglia volume over 2 years in patients with schizophrenia: typical versus atypical neuroleptics. *Am J Psychiat* 156: 1200-1204.
 12. Watanabe M and Munoz DP. (2010): Presetting basal ganglia for volitional actions. *J Neuroscience* 30 (30): 10144-10157.
 13. Graybiel AM. (1997): The basal ganglia and cognitive pattern generators. *Schizophrenia Bull* 23: 459-469.
 14. Frank MJ, Loughry B, and O'Reilly RC. (2001): Interactions between frontal cortex and basal ganglia in working memory: a computational model. *Cogn Affect Behav Ne* 1:137-160.
 15. Manoach DS, Ketwaroo GA, Polli FE, Thakkar KN, Barton JJS, Goff DC, *et al.* (2007): Reduced microstructural integrity of the white matter underlying anterior cingulate cortex is associated with increased saccadic latency in schizophrenia. *NeuroImage* 37: 599–610.
 16. Dyckman KA, Lee AKC, Agram Y, Vangel M, Goff DC, Barton JJS, *et al.* (2011): Abnormally persistent fMRI activation during antisaccades in schizophrenia: A neural correlate of perseveration? *Schizophr Res* 132: 62-68.

17. Connolly JD, Goodale MA, DeSouza JF, Menon RS, and Vilis T. (2000). A comparison of frontoparietal fMRI activation during anti-saccades and anti-pointing. *J Neurophysiol* 84: 1645–1655.
18. Drewes, J and VanRullen R. (2011): This is the rhythm of your eyes: the phase of ongoing electroencephalogram oscillations modulates saccadic reaction time. *J Neuroscience* 31: 4698-4708.
19. Hamm JP, Dyckman KA, McDowell JE, and Clementz BA. (2012): Pre-cue fronto-occipital alpha phase and distributed cortical oscillations predict failures of cognitive control. *J Neuroscience* 32: 7037-7041.
20. Schaeffer DJ, Rodrigue AL, Pierce JE, Unsworth N, Clementz BA, and McDowell JE. (2015): White matter structural integrity differs between people with schizophrenia and healthy groups as a function of cognitive control. *Schizophr Res* 169: 62-68.
21. Schaeffer DJ, Amlung MT, Li Q, Krafft CE, Austin BP, Dyckman KA, *et al.* (2013): Neural correlates of behavioral variation in healthy adults' antisaccade performance. *Psychophysiology* 50 (4): 325–333.
22. First MB, Spitzer RL, Gibbon M, and Williams JBW. (2002a): Structured clinical interview for DSM-IV-TR axis I disorders, research version, patient edition. (SCID-I/P) Biometrics Research. New York State Psychiatric Institute, New York (November).
23. First MB, Spitzer RL, Gibbon M, and Williams JBW. (2002b): Structured clinical interview for DSM-IV-TR axis I disorders, research version, non-patient edition. (SCID-I/NP) Biometrics Research. New York State Psychiatric Institute, New York (November).
24. Unsworth N, Heitz RP, Schrock JC, and Engle RW. (2005): An automated version of the operation span task. *Behav Res Methods* 37: 498–505.

25. Unsworth N and Spillers GJ. (2010): Working memory capacity: Attention control, secondary memory, or both? A direct test of the dual-component model. *J Mem Lang* 62: 392–406.
26. Unsworth N, Spillers GJ, and Brewer GA. (2012): The role of working memory capacity in autobiographical retrieval: individual differences in strategic search. *Memory* 20: 167–76.
27. Rorden C. (2007): DCM2NII (Version October 7) [Computer Software].
28. Smith SM. (2002): Fast robust automated brain extraction. *Hum Brain Mapp* 17 (3): 143–155.
29. Talarach J and Tournoux, P. (1998): Co-planar stereotaxic atlas of the human brain: A 3-dimensional proportional system, an approach to cerebral imaging. New York, NY: Thieme Medical Publishers.
30. Smith SM, Jenkinson M, Woolrich MW, Beckmann CF, Behrens TEJ, Johansen-Berg H, *et al.* (2004): Advances in functional and structural MR image analysis and implementation as FSL. *NeuroImage* 23: S208–S219.
31. Leemans A, Jeurissen B, Sijbers J, and Jones D. (2009): ExploreDTI: a graphical toolbox for processing, analyzing, and visualizing diffusion MR data. Paper Presented at the 17th Annual Meeting of Intl. Soc. Mag. Reson. Med. Hawaii, U.S.A.
32. Basser PJ, Pajevic S, Pierpaoli C, Duda J, and Aldroubi A. (2000): In vivo fiber tractography using DT-MRI data. *Magn Reson Med* 44: 625–632.
33. Leh SE, Ptito A, Chakravarty MM, and Strafella AP. (2007): Fronto-striatal connections in the human brain: A probabilistic diffusion tractography study. *Neurosci Lett* 419: 113–118.

34. Kane MJ, Bleckley MK, Conway ARA, and Engle RW. (2001): A controlled-attention view of working memory capacity. *J Exp Psychol: Gen* 2: 169-183.
35. Lebel C, Walker L, Leemans A, Phillips L, and Beaulieu C. (2008): Microstructural maturation of the human brain from childhood to adulthood. *NeuroImage* 40 (3): 1044–1055.
36. Song SK, Sun SW, Ramsbottom MJ, Chang C, Russell J, and Cross AH. (2002): Dysmyelination revealed through MRI as increased radial (but unchanged axial) diffusion of water. *NeuroImage* 17 (3): 1429–1436.
37. Lehericy S, Bardinet E, Tremblay L, Van de Moortele P, Pochon J, Dormont D, *et al.* (2006): Motor control in basal ganglia circuits using fMRI and brain atlas approaches. *Cereb Cortex* 16(2): 149-161.
38. Phillips JM and Everling S. (2012): Neural activity in the macaque putamen associated with saccades and behavioral outcome. *PLoS One* 7 (12): e51596.
39. Munoz DP and Everling S. (2004): Look away: The anti-saccade task and the voluntary control of eye movement. *Nat Rev Neurosci* 5: 218-228.

Table 4.1. Participant demographics.

	HCC	LCC	SZ
N	30	30	31
Age (years)	31.5 (12.7)	32.7 (10.7)	37.3 (9.5)
Gender (N female)	9	23	16
Handedness (N right, left, ambidextrous)	26, 3, 1	25, 5, 0	24, 4, 3
Anti-psychotic (atypical, typical, both; N on)	0, 0, 0	0, 0, 0	12, 3, 2
Anti-cholinergics (N on)	0	0	1
Anti-depressants (N on)	1	0	10
Anti-anxiety (N on)	1	0	0

Patient medication: 8 anti-psychotics only, 1 anti-psychotics and anti-cholinergics, 8 on anti-psychotics and anti-depressants, 2 anti-depressants only.

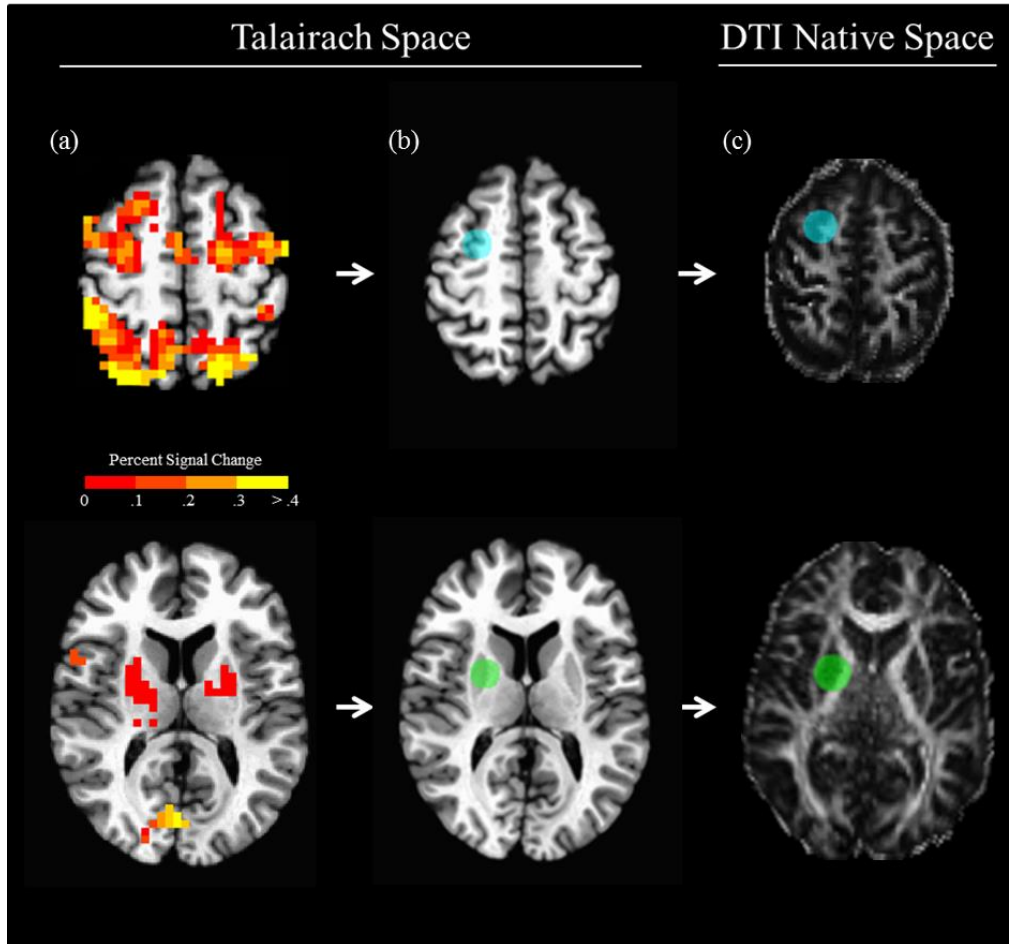


Figure 4.1: Transformation of fMRI regions of interest from Talairach space to DTI native space. (a) Shows BOLD percent signal change associated with a blocked-design antisaccade task ($\alpha = .05$, corrected) from an independent dataset (21) overlaid on a Talairach T1 image. Warmer colors represent greater BOLD percent signal change during antisaccade blocks. Regions of interest (8mm radii spheres) were drawn based on peak BOLD percent signal change in medial FEF (shown in top axial slice) and putamen (shown in bottom axial slice). (b) Shows resultant regions of interest in medial FEF (top, cyan) and putamen (bottom, green) overlaid on a Talairach T1 image. (c) Shows the same regions of interest after transformation to DTI native space of a representative subject, overlaid on a FA weighted image. Images displayed in radiological convention.

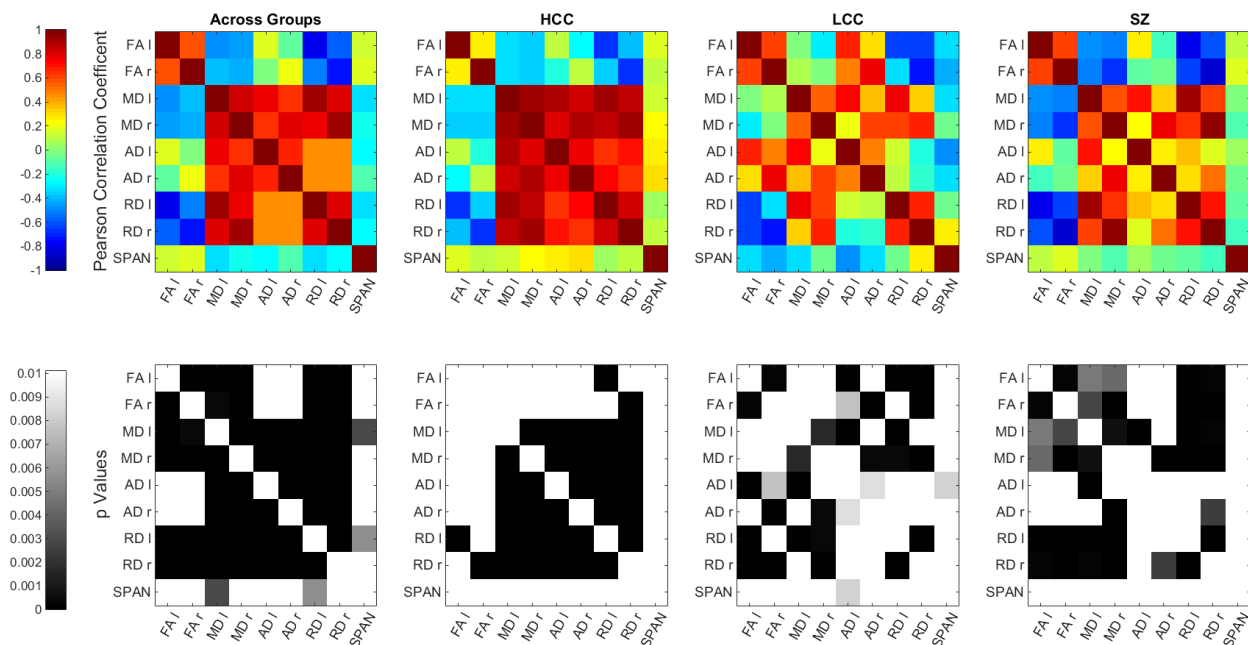


Figure 4.2: Brain and behavior correlations. Top row shows correlations between all measured variables across groups and for each group. Color scale represents the strength of the Pearson correlation coefficient for each comparison, with warmer colors indicating the strength of positive correlations and cooler colors indicating the strength of negative correlations. Bottom row shows the p value corresponding to the correlation values above; only shaded cells indicate a significant correlation at $\alpha = .01$ (.01 used to correct for multiple comparisons). Darker colors represent a lower p value than lighter colors. FA = fractional anisotropy; MD = mean diffusivity; AD = axial diffusivity; RD = radial diffusivity; SPAN = composite SPAN task score.

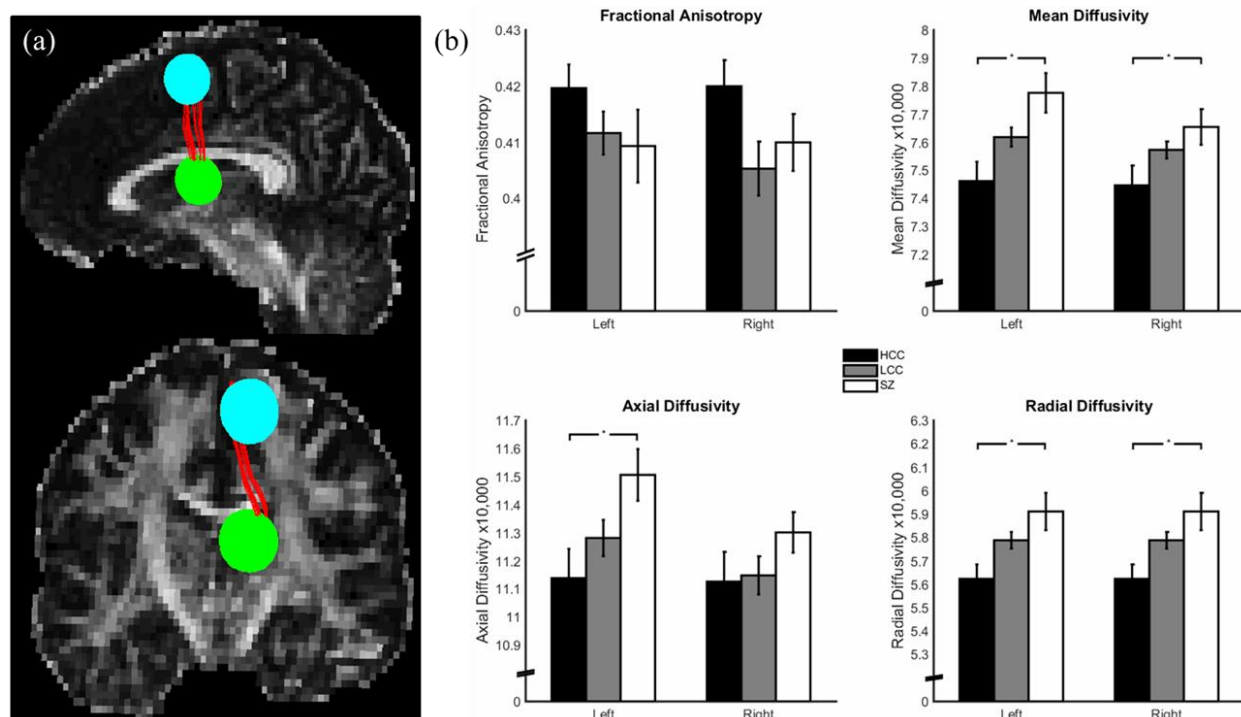


Figure 4.3: Fiber tracking between putamen and medial FEF. (a) Shows fibers (red, from a representative subject) tracked from putamen (green; seed region) to medial FEF (cyan) overlaid on a FA weighted image. (b) Shows measures of diffusivity drawn from the red fibers. Each subject contributed one value for each measure of diffusivity, with values averaged for each subject (i.e., all voxels containing red fibers contributed to one mean for each subject). Bar graphs show average (SE) diffusivity values for ipsilateral fiber connections between putamen and medial FEF. The SZ group showed higher bilateral mean diffusivity, left axial diffusivity, and bilateral radial diffusivity than the HCC group. The LCC group did not differ in any diffusivity values from the SZ or HCC groups. Mean, axial, and radial diffusivity values multiplied by 10,000. The black brackets with asterisks indicate a significant t tests between groups at $\alpha = .05$ (Tukey HSD multiple comparison corrected and controlled for age).

CHAPTER 5

DISCUSSION AND CONCLUSIONS

The focus of this body of work was to test for schizophrenia-specific alterations in saccadic eye movement circuitry. A long line of evidence suggests that people with schizophrenia have trouble with voluntary control of complex eye movements (Hutton & Ettinger, 2006). This deficit is mediated by cognitive control, a construct that refers to the ability to flexibly respond to changing environments (Alvarez & Emory, 2006). Cognitive control can be evoked with saccadic tasks by simply changing the instructions (e.g., look away from a cue, rather than toward it) – in doing so, the neural resources that support cognitive control are elicited and can be measured using functional imaging techniques. Although poor cognitive control performance in schizophrenia can be successfully modeled using complex saccadic tasks, some otherwise healthy subjects from the general population show poor performance on these tasks (albeit not as poor as schizophrenia; Hutton & Ettinger, 2006). Neuroimaging studies implicate similar structural and functional substrates with worse antisaccade error rates (i.e., lower cognitive control) in both healthy and schizophrenia samples (Camchong et al., 2006; Dyckman et al., 2007; Ford & Everling, 2009; Liu et al., 2013; Tu et al., 2010). As such, cognitive control ability may be a mediating factor in typical comparisons between healthy individuals and people with schizophrenia, with variance in functional and structural differences related to cognitive control rather than to the disease process of schizophrenia. In the present body of work, we demonstrated that the neural correlates underlying poor cognitive control

performance in schizophrenia do not significantly differ from patterns found in otherwise healthy individuals with low cognitive control.

In chapter 2, we demonstrated that patterns of activation associated with the antisaccade task differed between a healthy sample with high cognitive control (good performers) and a healthy sample with low cognitive control (poor performers). Specifically, these two groups elicited similar patterns of activation during correct trials, but different patterns during error trials. During error trials, the poor performers showed decreased activation in prefrontal cortex and posterior parietal cortex. These results are consistent with microelectrode and EEG data suggesting that the PFC sends top-down inhibitory signals directly to early visual areas, ostensibly preventing saccade errors toward the stimulus (Johnston & Everling, 2006; Munoz & Everling, 2004; Clementz et al., 2010). In addition to the PFC, parietal regions have been shown to play a role in top-down modulation of visual responses. Patients with parietal lesions show an increased rate of antisaccade errors (Sharpe et al., 2011). Thus, when top-down control regions are not active in poor performers, bottom-up visual regions (e.g., precuneus) are uninhibited, and the likelihood of making an antisaccade error is increased. Conversely, although good performers made errors, their top-down control circuitry was more active during the errors and likely contributed to a reduced probability of a future error.

Temporally rich probes of neural activity (e.g., EEG, electrophysiology) suggest that *when* regions are active plays an important role in correct execution of antisaccades. Parietal regions may be “pre-set” to preemptively re-map the target vector for antisaccade trials, as demonstrated with EEG – increases in alpha band phase locking have been shown to occur just before correct antisaccade trials, but this effect is absent just prior to error antisaccade trials (Hamm et al., 2012). Consistent with the human imaging evidence, electrophysiological

recordings of lateral intraparietal area in monkeys suggests that activity in the intraparietal area switches from the visual direction to the motor direction within 50 ms of the visual signal arriving at intraparietal area (Zhang & Barash, 2000). From these studies, we postulate that lower activation during error trials in the poor performers may actually represent the inability to recruit the neural resources necessary to pre-set regions to perform the antisaccade task correctly. Future studies probing individuals with low cognitive control using methods with greater temporal specificity would help to clarify this assertion.

These results are particularly interesting when considering comparisons between schizophrenia and healthy samples. The otherwise healthy sample with low cognitive control showed patterns of activation that resemble those associated with poor cognitive control performance in schizophrenia, with lower frontal and parietal activation associated with higher antisaccade error rates (Camchong et al., 2006; Dyckman et al., 2007; Ford & Everling, 2009; Tu et al., 2010). These results could suggest that functional alterations are not specific to the disease process of schizophrenia, but rather a function of decreased cognitive control capacity that is concomitant with the disease. To test this, as detailed in chapter 3, we recruited a schizophrenia sample to compare to two healthy samples – one with high levels of cognitive control (HCC) and another with low levels of cognitive control (LCC).

In chapter 3, we continued our examination of the neural correlates of poor cognitive control across healthy and schizophrenia groups by testing for differences in white matter structural integrity between the groups. DTI evidence suggests that deficits in cognitive control in people with schizophrenia are associated with white matter structural substrates across the brain (Liu et al., 2013), particularly in frontal and parietal regions (Karlsgodt et al., 2008). Similar frontal and parietal structures are implicated in poor cognitive control in healthy

individuals, with lower structural integrity linked to lower cognitive control scores (Burzynska et al., 2011). Accordingly, we hypothesized that white matter would differ in integrity (as measured by FA and RD) between HCC and the groups with low cognitive control (LCC and schizophrenia), but not between the schizophrenia and LCC groups, who show more similar cognitive control performance. Indeed, through the use of a whole-brain voxelwise analysis, we demonstrated widespread deficits in integrity between the schizophrenia group and HCC group, but not between the schizophrenia and LCC group. Although we expected whole brain differences in white matter integrity, we were specifically interested in the SLF because it is likely the main white matter conduit between the functional nodes that showed aberrant activity in chapter 2 (Burzynska et al., 2011; Schaeffer et al., 2013).

To test for differences in the SLF in chapter 3, we implemented a manual fiber tracking analysis. The benefit of using this type of analysis is that it mitigates the effect of spatial transformation on the data. In healthy samples, voxelwise approaches are subject to partial volume effects and misregistration; in patient samples, these problems are compounded if the patient group has differences in morphology (i.e., the tract has disease related idiosyncrasies that are lost in transformation). Indeed, people with schizophrenia show differences in structural morphology across the brain (Corson, Nopoulos, Miller, Arndt, & Andreasen, 1999). Thus, fiber tracking allowed us to test a specific hypothesis (that SLF would differ between the groups) by isolating that tract directly in each individual. The results demonstrated highly concordant results ($r = .82$) with the voxelwise analysis, wherein the schizophrenia group showed decreased FA and increased RD compared to the HCC group, a pattern indicative of less axonal coherence and myelination (Lebel et al., 2008; Song et al., 2002). Finding lower white matter integrity in the schizophrenia group is consistent with evidence suggesting that white matter integrity of the SLF

modulates cognitive control performance (Burzynska et al., 2011). These results further confirmed our suspicion that these alterations are not specific to the disease process of schizophrenia, but rather a function of decreased cognitive control capacity that is concomitant with the disease.

In chapter 4, we combined the data from chapters 2 and 3 in the pursuit of testing for alterations in the white matter fibers that serve to connect functional nodes of the saccadic eye movement network. Specifically, we used the fMRI data from chapter 2 to isolate two functional nodes of the saccadic eye movement network implicated in poor antisaccade performance in schizophrenia – putamen of the basal ganglia and medial FEF. These regions were chosen in part because of their importance in antisaccade performance, but also because these are some of the only fibers tracked to date using this method (but only in a healthy sample; Neggers et al., 2012). Accordingly, we sought to replicate results shown in Neggers et al. (2012) in our healthy sample, and extend these findings by applying this methodology to a sample with schizophrenia. Similar to Neggers et al. (2012), our results demonstrated white matter fiber connections between putamen and medial FEF in both healthy and schizophrenia samples. Although DTI does not delineate between anterograde and retrograde connections, these fibers are ostensibly part of feed-forward and feed-back loops between putamen and cortical areas (in this case, medial FEF). In the context of saccadic eye movements, these loops likely play a role in cognitive control by presetting the oculomotor system to perform the antisaccade task correctly – i.e. inhibiting a reflexive saccade and executing a volitional saccade away from the cue (Neggers et al., 2012; Raemaekers et al., 2002).

Consistent with the results from chapter 3, the results in chapter 4 demonstrated lower white matter integrity (as marked by higher MD and RD) in the schizophrenia group than in the

HCC group, but not the LCC group who showed similarly poor cognitive control performance. Again, these results supported our overarching hypothesis that white matter alterations are not specific to the disease process of schizophrenia, but rather a function of decreased cognitive control capacity that is concomitant with the disease. Future studies may build on these results by tracking fibers between other nodes of the saccadic network; understanding how functional and structural substrates interact to result in poor antisaccade performance will help elucidate the mechanisms of poor cognitive control in healthy and diseased states.

Conclusion

Although antisaccade performance has been presented as a reliable and robust endophenotype for schizophrenia (Radant et al., 2015), the present body of work provides evidence to suggest that the neural correlates underlying poor antisaccade performance in schizophrenia do not drastically differ from healthy individuals who perform poorly on the antisaccade task. As demonstrated in chapter 3, cognitive control deficits seem to vary linearly with connectivity across the brain, suggesting that poor cognitive control in schizophrenia is likely the result of network dysfunction, rather than any one region going awry during the development or disease process of schizophrenia. Interestingly, recent genetic evidence suggests that schizophrenia may arise from excessive synaptic pruning by microglia during adolescence or early adulthood (Sekar, 2016). Although far from demonstrating etiology, this evidence fits well with extant neuroimaging data in schizophrenia, which shows dysfunctional integration across multiple neuronal systems (Friston, 1999). During development, excessive neuronal pruning may result in underdevelopment of connectivity, altering the dynamics of network communication in schizophrenia.

In conclusion, saccadic eye movement paradigms are a useful tool for probing aberrant neural circuitry in schizophrenia. Neuroimaging studies aimed at determining schizophrenia specific alterations in functional and structural circuitry schizophrenia may aid in characterizing phenotypes of schizophrenia. The present results highlight the use of a behaviorally matched comparison group in neuroimaging studies – future studies might reduce confounding variance in their results by matching schizophrenia groups to healthy groups with similar levels of cognitive control. Increasing the specificity of schizophrenia-healthy comparisons may ultimately lead to a better understanding of the pathophysiology underlying this devastating disorder.

REFERENCES

- Abrams, R. A., Meyer, D. E., & Kornblum, S. (1989). Speed and accuracy of saccadic eye movements: Characteristics of impulse variability in the oculomotor system. *Journal of Experimental Psychology: Human Perception and Performance*, *15*, 529–543.
- Alvarez, J. A., & Emory, E. (2006). Executive function and the frontal lobes: A meta-analytic review. *Neuropsychology Review*, *16*, 17-42.
- American Psychiatric Association. (2013). *Diagnostic and statistical manual of mental disorders* (5th ed.). Washington, DC: Author.
- Blanke, O., & Seeck, M. (2003). Direction of saccadic and smooth eye movements induced by electrical stimulation of the human frontal eye field: effect of orbital position. *Experimental Brain Research*, *150*, 174–83.
- Brown, M. R. G., DeSouza, J. F. X., Goltz, H. C., Ford, K., Menon, R. S., Goodale, M. A., & Everling, S. (2004). Comparison of memory and visually guided saccades using event-related fMRI. *Journal of Neurophysiology*, *91*, 873–89.
- Burzynska, A. Z., Nagel, I. E., Preuschhof, C., Li, S. C., Lindenberger, U., Bäckman, L., & Heekeren, H. R. (2011). Microstructure of frontoparietal connections predicts cortical responsivity and working memory performance. *Cerebral Cortex*, *21*, 2261–71.
- Calkins, M. E., Curtis, C. E., Iacono, W. G., & Grove, W. M. (2004). Antisaccade performance is impaired in medically and psychiatrically healthy biological relatives of schizophrenia patients. *Schizophrenia Research*, *71*, 167–78.

- Camchong, J., Dyckman, K. A., Chapman, C. E., Yanasak, N. E., & McDowell, J. E. (2006). Basal ganglia-thalamocortical circuitry disruptions in schizophrenia during delayed response tasks. *Biological Psychiatry, 60*, 235–41.
- Chan, F., Armstrong, I. T., Pari, G., Riopelle, R. J., & Munoz, D. P. (2005). Deficits in saccadic eye-movement control in Parkinson's disease. *Neuropsychologia, 43*, 784–96.
- Connolly, J. D., Goodale, M. A., DeSouza, J. F., Menon, R. S., & Vilis, T. (2000). A comparison of frontoparietal fMRI activation during anti-saccades and anti-pointing. *Journal of Neurophysiology, 84*, 1645–55.
- Corson, P. W., Nopoulos, P., Miller, D. D., Arndt, S., & Andreasen, N. C. (1999). Change in basal ganglia volume over 2 years in patients with schizophrenia: typical versus atypical neuroleptics. *American Journal of Psychiatry, 156*, 1200-1204.
- Curtis, C. E., & D'Esposito, M. (2003). Success and failure suppressing reflexive behavior. *Journal of Cognitive Neuroscience, 15*, 409–418.
- Cutsuridis, V., Kumari, V., & Ettinger, U. (2014). Antisaccade performance in schizophrenia: a neural model of decision making in the superior colliculus. *Frontiers in Neuroscience, 8*, 13.
- De Weijer, A. D., Mandl, R. C. W., Sommer, I. E. C., Vink, M., Kahn, R. S., & Nieuwenhuis, S. F. W. (2010). Human fronto-tectal and fronto-striatal-tectal pathways activate differently during anti-saccades. *Frontiers in Human Neuroscience, 4*, 41.
- DeSouza, J. F. X., Menon, R. S., & Everling, S. (2003). Preparatory set associated with pro-saccades and anti-saccades in humans investigated with event-related fMRI. *Journal of Neurophysiology, 89*, 1016–23.

- Doricchi, F., & Tomaiuolo, F. (2003). The anatomy of neglect without hemianopia: a key role for parietal-frontal disconnection? *Neuroreport*, *14*, 2239–43.
- Draganski, B., Kherif, F., Klöppel, S., Cook, P. A., Alexander, D. C., Parker, G. J. M., ... Frackowiak, R. S. J. (2008). Evidence for segregated and integrative connectivity patterns in the human Basal Ganglia. *The Journal of Neuroscience*, *28*, 7143–52.
- Duchowski, A. T. (2007). *Eye tracking methodology: theory and practice* (Second). Springer.
- Dyckman, K. A., Camchong, J., Clementz, B. A., & McDowell, J. E. (2007). An effect of context on saccade-related behavior and brain activity. *NeuroImage*, *36*, 774–84.
- Ettinger, U., Kumari, V., Crawford, T. J., Davis, R. E., Sharma, T., & Corr, P. J. (2003). Reliability of smooth pursuit, fixation, and saccadic eye movements. *Clinical Neuroscience Research*, *40*, 620–628.
- Evdokimidis, I., Smyrnis, N., Constantinidis, T. S., Stefanis, N. C., Avramopoulos, D., Paximadis, C., ... Stefanis, C. N. (2002). The antisaccade task in a sample of 2,006 young men. I. Normal population characteristics. *Experimental Brain Research*, *147*, 45–52.
- Everling, S., & Fischer, B. (1998). The antisaccade: a review of basic research and clinical studies. *Neuropsychologia*, *36*, 885–899.
- Fjell, A. M., Westlye, L. T., Greve, D. N., Fischl, B., Benner, T., van der Kouwe, A. J. W., ... Walhovd, K. B. (2008). The relationship between diffusion tensor imaging and volumetry as measures of white matter properties. *NeuroImage*, *42*, 1654–68.
- Ford, K. A., & Everling, S. (2009). Neural activity in primate caudate nucleus associated with pro- and antisaccades. *Journal of Neurophysiology*, *102*, 2334–41.

- Ford, K. A., Goltz, H. C., Brown, M. R. G., & Everling, S. (2005). Neural processes associated with antisaccade task performance investigated with event-related fMRI. *Journal of Neurophysiology*, *94*, 429–440.
- Friston, K. J. (1998). The disconnection hypothesis. *Schizophrenia Research*, *30*, 115–125.
- Fukumoto-Motoshita, M., Matsuura, M., Ohkubo, T., Ohkubo, H., Kanaka, N., Matsushima, E., ... Matsuda, T. (2009). Hyperfrontality in patients with schizophrenia during saccade and antisaccade tasks: a study with fMRI. *Psychiatry and Clinical Neurosciences*, *63*, 209–17.
- Fukushima, J., Fukushima, K., Chiba, T., Tanaka, S., Yamashita, I., & Kato, M. (1988). Disturbances of voluntary control of saccadic eye movements in schizophrenic patients. *Biological Psychiatry*, *23*, 670–7.
- Gaymard, B., Pierrot-Deseilligny, C., & Rivaud, S. (1990). Impairment of sequences of memory-guided saccades after supplementary motor area lesions. *Annals of Neurology*, *28*, 622–6.
- Geng, J. J., Ruff, C. C., & Driver, J. (2009). Saccades to a remembered location elicit spatially specific activation in human retinotopic visual cortex. *Journal of Cognitive Neuroscience*, *21*, 230–45.
- Girard, B., & Berthoz, A.. (2005). From brainstem to cortex: computational models of saccade generation circuitry. *Progress in Neurobiology*, *77*, 215–51.
- Goldberg, M. E., & Wurtz, R. H. (2013). Visual Processing and Action. In E. R. Kandel, J. H. Schwartz, T. M. Jessel, S. A. Siegelbaum, & A. J. Hudspeth (Eds.), *Principles of Neural Science* (5th ed.).
- Goldman-Rakic, P. S. (1994). Working memory dysfunction in schizophrenia. *Journal of Neuropsychiatry Clinical Neuroscience*, *6*, 348–357.

- Greenberg, A. S., Verstynen, T., Chiu, Y. C., Yantis, S., Schneider, W., & Behrmann, M. (2012). Visuotopic cortical connectivity underlying attention revealed with white-matter tractography. *The Journal of Neuroscience*, *32*, 2773–82.
- Greenlee, M. (2000). Human cortical areas underlying the perception of optic flow: brain imaging studies. *Int Rev Neurobiol*, *207*, 269–292.
- Hallett, P. E. (1977). Primary and secondary saccades to goals defined by instructions. *Vision Research*, *18*, 1279–1296.
- Heide, W., Binkofski, F., Seitz, R. J., Posse, S., Nitschke, M. F., Freund, H. J., & Kömpf, D. (2001). Activation of frontoparietal cortices during memorized triple-step sequences of saccadic eye movements: an fMRI study. *The European Journal of Neuroscience*, *13*, 1177–89.
- Hoefl, F., Barnea-Goraly, N., Haas, B. W., Golarai, G., Ng, D., Mills, D., ... Reiss, A. L. (2007). More is not always better: increased fractional anisotropy of superior longitudinal fasciculus associated with poor visuospatial abilities in Williams syndrome. *The Journal of Neuroscience*, *27*, 11960–5.
- Holzman, P. S., Proctor, L. R., & Hughes, D. W. (1973). Eye-tracking patterns in schizophrenia. *Science*, *181*, 179–181.
- Hua, K., Zhang, J., Wakana, S., Jiang, H., Li, X., Reich, D. S., ... Mori, S. (2008). Tract probability maps in stereotaxic spaces: analyses of white matter anatomy and tract-specific quantification. *NeuroImage*, *39*, 336–47.
- Hutton, S. B., & Ettinger, U. (2006). The antisaccade task as a research tool in psychopathology: a critical review. *Psychophysiology*, *43*, 302–13.

- Ito, S., Stuphorn, V., Brown, J. W., & Schall, J. D. (2003). Performance monitoring by the anterior cingulate cortex during saccade countermanding. *Science*, *302*, 120–2.
- Jamadar, S. D., Fielding, J., & Egan, G. F. (2013). Quantitative meta-analysis of fMRI and PET studies reveals consistent activation in fronto-striatal-parietal regions and cerebellum during antisaccades and prosaccades. *Frontiers in Psychology*, *4*, 749.
- Jang, S. H., & Hong, J. H. (2012). The anatomical characteristics of superior longitudinal fasciculus I in human brain: Diffusion tensor tractography study. *Neuroscience Letters*, *506*, 146–148.
- Jiang, H., van Zijl, P. C. M., Kim, J., Pearlson, G. D., & Mori, S. (2006). DtiStudio: resource program for diffusion tensor computation and fiber bundle tracking. *Computer Methods and Programs in Biomedicine*, *81*, 106–16.
- Jones, D., & Leemans, A. (2011). Diffusion Tensor Imaging. In M. Modo & J. Bulte (Eds.), *Magnetic Resonance Neuroimaging* (1st ed., pp. 127–144). CRC Press.
- Kapoula, Z., Isotalo, E., Müri, R. M., Bucci, M. P., & Rivaud-Péchoix, S. (2001). Effects of transcranial magnetic stimulation of the posterior parietal cortex on saccades and vergence. *Neuroreport*, *12*, 4041–6.
- Karlsgodt, K. H., van Erp, T. G. M., Poldrack, R. A., Bearden, C. E., Nuechterlein, K. H., & Cannon, T. D. (2008). Diffusion tensor imaging of the superior longitudinal fasciculus and working memory in recent-onset schizophrenia. *Biological Psychiatry*, *63*, 512–8.
- Keshavan, M. S., Clementz, B. A., Pearlson, G. D., Sweeny, J. A., & Tamminga, C. A. (2013). Reimagining psychoses: an agnostic approach to diagnosis. *Schizophrenia Research*, *146*, 10-16.

- Krafft, C., Schwarz, N., Chi, L., Li, Q., Schaeffer, D., Rodrigue, A. L., . . . McDowell, J. (2012). The location and function of parietal cortex supporting of reflexive and volitional saccades, a meta-analysis of over a decade of functional MRI data. In A. Costa & E. Villalba (Eds.), *Horizons of neuroscience research*, volume 9 (pp. 131–153). Hauppauge, NY: Nova Science Publishers.
- Kubicki, M., McCarley, R., Westin, C. F., Park, H. J., Maier, S., Kikinis, R., . . . Shenton, M. E. (2007). A review of diffusion tensor imaging studies in schizophrenia. *Journal of Psychiatric Research*, *41*, 15–30.
- Leemans, A., Jeurissen, B., Sijbers, J., & Jones, D. (2009). ExploreDTI: a graphical toolbox for processing, analyzing, and visualizing diffusion MR data. In *Paper presented at the 17th Annual Meeting of Intl Soc Mag Reson Med*. Hawaii, U.S.A.
- Lehéricy, S., Bardinet, E., Tremblay, L., Van de Moortele, P.F., Pochon, J.B., Dormont, D., . . . Ugurbil, K. (2006). Motor control in basal ganglia circuits using fMRI and brain atlas approaches. *Cerebral Cortex*, *16*, 149–61.
- Leigh, R. J., & Kennard, C. (2004). Using saccades as a research tool in the clinical neurosciences. *Brain : A Journal of Neurology*, *127*, 460–77.
- Leigh, R. J., & Zee, D. S. (2006). *The Neurology of Eye Movements* (4th ed.). New York: Oxford University Press, Inc.
- Lewis, J. W., & Van Essen, D. C. (2000). Corticocortical connections of visual, sensorimotor, and multimodal processing areas in the parietal lobe of the macaque monkey. *The Journal of Comparative Neurology*, *428*, 112–37.
- Levin, S., Holzman, P. S., Rothenberg, S. J., & Lipton, R. B. (1981). Saccadic eye movements in psychotic patients. *Psychiatry Research*, *58*, 47–58.

- Liu, X., Lai, Y., Wang, X., Hao, C., Chen, L., Zhou, Z., ... Hong, N. (2013). Reduced white matter integrity and cognitive deficit in never-medicated chronic schizophrenia: a diffusion tensor study using TBSS. *Behavioural Brain Research*, 252, 157–63.
- Mabbott, D. J., Rovet, J., Noseworthy, M. D., Smith, M. Lou, & Rockel, C. (2009). The relations between white matter and declarative memory in older children and adolescents. *Brain Research*, 1294, 80–90.
- Makris, N., Kennedy, D. N., McInerney, S., Sorensen, a G., Wang, R., Caviness, V. S., & Pandya, D. N. (2005). Segmentation of subcomponents within the superior longitudinal fascicle in humans: a quantitative, in vivo, DT-MRI study. *Cerebral Cortex*, 15, 854–69.
- Manoach, D. S., Ketwaroo, G. A., Polli, F. E., Thakkar, K. N., Barton, J. J. S., Goff, D. C., ... Tuch, D. S. (2007). Reduced microstructural integrity of the white matter underlying anterior cingulate cortex is associated with increased saccadic latency in schizophrenia. *NeuroImage*, 37, 599–610.
- Matsuda, T., Matsuura, M., Ohkubo, T., Ohkubo, H., Matsushima, E., Inoue, K., ... Kojima, T. (2004). Functional MRI mapping of brain activation during visually guided saccades and antisaccades: cortical and subcortical networks. *Psychiatry Research*, 131, 147–55.
- McDowell, J. E., Brown, G. G., Paulus, M., Martinez, A., Stewart, S. E., Dubowitz, D. J., & Braff, D. L. (2002). Neural correlates of refixation saccades and antisaccades in normal and schizophrenia subjects. *Biological Psychiatry*, 51, 216–223.
- Mcdowell, J. E., Dyckman, K. A., Austin, B., & Clementz, B. A. (2009). Saccades : Evidence from Studies of Humans, 68, 255–270.

- McDowell, J. E., Myles-Worsley, M., Coon, H., Byerley, W., & Clementz, B. A. (1999). Measuring liability for schizophrenia using optimized antisaccade stimulus parameters. *Psychophysiology*, *36*, 138–141.
- Merriam, E. P., Genovese, C. R., & Colby, C. L. (2007). Remapping in human visual cortex. *Journal of Neurophysiology*, *97*, 1738–1755.
- Mostofsky, S. H., Lasker, A. G., Cutting, L. E., Denckla, M. B., & Zee, D. S. (2001). Oculomotor abnormalities in attention deficit hyperactivity disorder: a preliminary study. *Neurology*, *57*, 423–30.
- Müller, N., Riedel, M., Eggert, T., & Straube, A. (1999). Internally and externally guided voluntary saccades in unmedicated and medicated schizophrenic patients. Part II. Saccadic latency, gain, and fixation suppression errors. *European Archives of Psychiatry and Clinical Neuroscience*, *249*, 7–14.
- Munoz, D. P., & Everling, S. (2004). Look away: the anti-saccade task and the voluntary control of eye movement. *Nature Reviews. Neuroscience*, *5*, 218–28.
- Müri, R. M., Rösler, K. M., & Hess, C. W. (1994). Influence of transcranial magnetic stimulation on the execution of memorised sequences of saccades in man. *Experimental Brain Research*, *101*, 521–4.
- Nakashima, Y., Momose, T., Sano, I., Katayama, S., Nakajima, T., Shin-Ichi, N., & Matsushita, M. (1994). Cortical control of saccade in normal and schizophrenic subjects: A PET study using a task-evoked rCBF paradigm. *Schizophrenia Research*, *12*, 125–264.
- Neggers, S. F. W., Diepen, R. M. Van, Zandbelt, B. B., Vink, M., Mandl, R. C. W., & Gutteling, T. P. (2012). A functional and structural investigation of the human fronto-basal volitional saccade network. *PloS One*, *7*, e29517.

- Petit, L., Orssaud, C., Tzourio, N., Salamon, G., Mazoyer, B., & Berthoz, A. (1993). PET study of voluntary saccadic eye movements in humans: Basal system and cingulate cortex involvement, *Journal of Neurophysiology*, *69*, 1009-17.
- Pierrot-Deseilligny, C. (2003). Decisional role of the dorsolateral prefrontal cortex in ocular motor behaviour. *Brain*, *126*, 1460–1473.
- Pierrot-deseilligny, C. H., Ploner, C. J., Müri, R. M., & Gaymard, B. (2002). Effects of Cortical Lesions on Saccadic Eye Movements in Humans, *229*, 216–229.
- Pierrot-Deseilligny, C., Milea, D., & Müri, R. (2004). Eye movement control by the cerebral cortex. *Current Opinion in Neurology*, *17*, 17–25.
- Pierrot-Deseilligny, C., Ploner, C. J., Gaymard, B., Demeret, S., Mu, R. M., & Neurologie, È. (2003). Decisional role of the dorsolateral prefrontal cortex in ocular motor behaviour. *Brain*, *126*, 1460–1473.
- Poldrack, R. A., & Mumford, J. A. (2009). Independence in ROI analysis: Where is the voodoo? *Social Cognitive and Affective Neuroscience*, *4*, 208–213.
- Radant, A. D., Millard, S. P., Braff, D. L., Calkins, M. E., Dobie, D. J., Freedman, R., ... Tsuang, D. W. (2015). Robust differences in antisaccade performance exist between COGS schizophrenia cases and controls regardless of recruitment strategies. *Schizophrenia Research*, *163*, 47-52.
- Raemaekers, M., Vink, M., Zandbelt, B., van Wezel, R. J. A., Kahn, R. S., & Ramsey, N. F. (2007). Test-retest reliability of fMRI activation during prosaccades and antisaccades. *NeuroImage*, *36*, 532–42.
- Rorden, C. (2007). DCM2NII (Version October 7) [Computer Software].

- Salzman, C. D., & Newsome, W. T. (1994). Neural mechanisms for forming a perceptual decision. *Science*, *264*, 231–237.
- Schaeffer, D. J., Amlung, M. T., Li, Q., Krafft, C. E., Austin, B. P., Dyckman, K. a, & McDowell, J. E. (2013). Neural correlates of behavioral variation in healthy adults' antisaccade performance. *Psychophysiology*, *50*, 325–33.
- Schaeffer, D. J., Rodrigue, A. L., Pierce, J. E., Clementz, B. A., & McDowell, J. E. (2014). Diffusion tensor imaging reveals structural differences related to antisaccade performance in people with schizophrenia. In *Cognitive Neuroscience Society*.
- Schlag, J., & Schlag-Rey, M. (1987). Evidence for a supplementary eye field. *Journal of Neurophysiology*, *57*, 179–200.
- Schlag-Rey, M., Amador, N., Sanchez, H., & Schlag, J. (1997). Antisaccade performance predicted by neuronal activity in the supplementary eye field. *Nature*, *390*, 398–401.
- Sekar, A., Bialas, A. R., de Rivera, H., Davis, A., Hammond, T. R., Kamitaki, N., ... McCarroll, S. A. (2016). Schizophrenia risk from complex variation of complement component 4. *Nature*, *530*, 177-183.
- Smith, S. M. (2002). Fast robust automated brain extraction. *Human Brain Mapping*, *17*, 143–55.
- Smith, S. M., Jenkinson, M., Johansen-Berg, H., Rueckert, D., Nichols, T. E., Mackay, C. E., ... Behrens, T. E. J. (2006). Tract-based spatial statistics: voxelwise analysis of multi-subject diffusion data. *NeuroImage*, *31*, 1487–505.
- Smith, S. M., Jenkinson, M., Woolrich, M. W., Beckmann, C. F., Behrens, T. E. J., Johansen-Berg, H., ... Matthews, P. M. (2004). Advances in functional and structural MR image analysis and implementation as FSL. *NeuroImage*, *23*, S208–19.

Song, S.K., Sun, S.W., Ramsbottom, M. J., Chang, C., Russell, J., & Cross, A. H. (2002).

Dysmyelination revealed through MRI as increased radial (but unchanged axial) diffusion of water. *NeuroImage*, *17*, 1429–36.

Stufflebeam, S. M., Witzel, T., Mikulski, S., Hämäläinen, M. S., Temereanca, S., Barton, J. J. S.,

... Manoach, D. S. (2008). A non-invasive method to relate the timing of neural activity to white matter microstructural integrity. *NeuroImage*, *42*, 710–716.

Tanji, J. (2001). Sequential organization of multiple movements: involvement of cortical motor

areas. *Annual Review of Neuroscience*, *24*, 631–651.

Tanner, J. E., & Stejskal, E. O. (1968). Spin diffusion measurements: Spin echoes in the

ofatimedependent field gradient. *Journal of Chemical Physics*, *49*, 1768–1777.

Taylor, A. J. G., & Hutton, S. B. (2007). The effects of individual differences on cued

antisaccade performance. *Journal of Eye Movment Research*, *1*, 1–9.

Tu, P., Buckner, R. L., Zollei, L., Dyckman, K. a, Goff, D. C., & Manoach, D. S. (2010).

Reduced functional connectivity in a right-hemisphere network for volitional ocular motor control in schizophrenia. *Brain* , *133*, 625–37.

Unsworth, N., Heitz, R. P., Schrock, J. C., & Engle, R. W. (2005). An automated version of the

operation span task. *Behavior Research Methods*, *37*, 498–505.

Unsworth, N., & Spillers, G. J. (2010). Working memory capacity: Attention control, secondary

memory, or both? A direct test of the dual-component model. *Journal of Memory and Language*, *62*, 392–406.

Unsworth, N., Spillers, G. J., & Brewer, G. A. (2012). The role of working memory capacity in

autobiographical retrieval: individual differences in strategic search. *Memory*, *20*, 167–76.

- Wakana, S., Caprihan, A., Panzenboeck, M. M., Fallon, J. H., Perry, M., Gollub, R. L., ... Mori, S. (2007). Reproducibility of quantitative tractography methods applied to cerebral white matter. *NeuroImage*, *36*, 630–44.
- Walter, M., Stadler, J., Tempelmann, C., Speck, O., & Northoff, G. (2008). High resolution fMRI of subcortical regions during visual erotic stimulation at 7 T. *Magn Reson Mater Phy*, *21*, 103–11.
- Watanabe, M., & Munoz, D. P. (2010). Presetting basal ganglia for volitional actions. *The Journal of Neuroscience*, *30*, 10144–57.
- Whitford, T. J., Kubicki, M., & Shenton, M. E. (2011). Diffusion tensor imaging, structural connectivity, and schizophrenia. *Schizophrenia Research and Treatment*, *2011*, 1-7.
- Zhang, M., & Barash, S. (2000). Neuronal switching of sensorimotor transformations for antisaccades. *Nature*, *408*, 971–5.